

Therapeutic role of mesenchymal stem cells in carbon tetrachloride- induced hepatic pathogenesis in the adult male albino rat: A microscopic and biochemical study.

Hafyz Waly Attallah¹; Safwat Wadie Gerges¹; Laila Ahmed Rashed²; Maha Khaled Abd-El-Wahed³; Radwa Mohamed El-Sayed³

¹Anatomy and Embryology Department, Faculty of Medicine, Cairo University, Cairo, Egypt

²Biochemistry and Molecular Biology Department, Faculty of Medicine, Cairo University, Cairo, Egypt

³Anatomy and Embryology Department, Faculty of Medicine, Fayoum University, Fayoum, Egypt

mahakhaled007@yahoo.com

Abstract: The aim of the present work is to evaluate the possible therapeutic role of intravenous administration of mesenchymal stem cells against CCL4-induced hepatotoxic changes. Hepatotoxicity was induced in this study by injection of carbon tetrachloride (CCl₄) subcutaneously at a dose of 0.2 ml/kg body weight twice weekly for four and eight weeks durations. Another two groups were injected with CCl₄ for four and eight weeks then left to observe the effect of spontaneous recovery after four weeks. Bone marrow derived mesenchymal stem cells (MSC) were injected into the tail vein at a dose of 1x10⁶ stem cells labeled with PKH26 dye in 1 ml phosphate buffer saline in two groups after injected with CCl₄ for four and eight weeks. Liver specimens were examined by both light and transmission electron microscopic methods. Different levels of liver enzymes (ALT, AST and GGT) were measured. This study revealed that intravenous injection of MSC was more effective in rescuing liver failure than spontaneous recovery and could be used as a suitable line of therapy than liver transplantation in end-stage liver disease.

[Hafyz Waly Attallah; Safwat Wadie Gerges; Laila Ahmed Rashed; Maha Khaled Abd-El-Wahed; Radwa Mohamed El-Sayed. **Therapeutic role of mesenchymal stem cells in carbon tetrachloride- induced hepatic pathogenesis in the adult male albino rat: A microscopic and biochemical study.** *J Am Sci* 2017;13(6):30-52]. ISSN 1545-1003 (print); ISSN 2375-7264 (online). <http://www.jofamericanscience.org>. 5. doi:[10.7537/marsjas130617.05](https://doi.org/10.7537/marsjas130617.05).

Key words: Hepatotoxicity, Carbon tetrachloride (CCl₄), Mesenchymal stem cells (MSC).

1. Introduction:

Cirrhosis is defined as a diffuse process inducing fibrosis and nodule formation. It is the final changes of the fibrogenesis consequent to chronic liver injury (*Dooley et al., 2011*).

There are four structural components of the liver: primarily, the liver parenchyma consists of plates of liver cells (hepatocytes). Secondly, connective tissue stroma that is continuous with the fibrous capsule of Glisson. Blood vessels (arteries and veins), nerves, lymphatic vessels and bile ducts travel within the connective tissue stroma. Thirdly, sinusoidal capillaries (hepatic sinusoids), the vascular channels between the plates of hepatocytes and finally, the perisinusoidal space (space of Disse) which lies between the hepatocytes and the interrupted sinusoidal endothelium (*Ross and Pawlina, 2011*). The sinusoids are lined by endothelial cells (with small pores; fenestrae) for macromolecule diffusion from blood to hepatocytes. On the luminal side of the sinusoidal endothelium are the phagocytic cells of the reticulo-endothelial system (Kupffer cells) and pit cells with natural killer function (*Greets, 2001*).

There are three concepts to describe the structure of the hepatic functional units (*Ross and Pawlina, 2011*). The classic hepatic lobule concept based on structural parameters *Kierszenbaum (2002)*. The portal lobule concept based on the bile drainage

pathway from adjacent lobules toward the same bile duct (*Steven and Lowe, 2005*) and the liver acinus concept based on the gradient distribution of oxygen along the venous sinusoids of adjacent lobule (*Junqueira and Carneiro, 2005*).

Concerning ultrastructure of liver, the hepatocyte is polyhedral; it is described as having six surfaces. Two of its surfaces face the perisinusoidal space of Disse. The plasma membrane of two surfaces faces hepatocytes. The remaining two surfaces face bile canaliculi (*Theard et al., 2007*). The hepatocytes have abundant cytoplasmic organelles spherical to ovoid mitochondria, electron dense lysosomes, Golgi apparatus and parallel cisternae of smooth and rough endoplasmic reticulum covered by ribosomes. (*Das et al., 2013*).

Carbon tetrachloride (CCl₄) is the common name for tetra chloromethane, a nonflammable, volatile liquid that has a high vapour density. In liquid form it is clear, colourless, and has a characteristic odor. CCl₄ has been used as a dry cleaning agent and fire extinguisher material. It has also been used as a solvent for rubber cement as well as for cleaning equipment and machinery. Further uses include those of a refrigerant and as a feedstock chemical for fluorocarbon propellants (*Lide, 2006*). Due to its high lipid solubility, it is readily absorbed through

inhalation, ingestion, and possibly by dermal contact with the liquid form (*Walker et al., 2001*).

Zowail et al. (2012) reported that eight weeks after CCl₄ administration to rats, the liver appeared with marked pathological changes where some hepatocytes showed complete destruction with pyknosis of their nuclei and presence of inclusions inside the cytoplasm indicating irreversible stage of cell death. Other hepatocytes showed depletion of the membranous organelles.

Smyth et al. (2007) found that repeated administration of CCl₄ leads to significant elevation of plasma liver enzymes activity (transaminases, gamma glutamyl transferase).

The mechanism of these liver changes could be attributed to the fact that CCl₄ is bio-transformed by the cytochrome P450 system in the mitochondria to produce the highly reactive trichloro-methyl free radical (CCl₃). This free radical then combined with cellular lipids and proteins in the presence of oxygen to form a trichloromethyl peroxy radical, which may attack lipids on the membrane of endoplasmic reticulum faster than CCl₃. Thus CCl₃ elicited lipid peroxidation (*Mohona-Rao et al., 2006*).

Xiao et al. (2012) suggested that reactive oxygen species (ROS) cause oxidative stress in the liver and attack several cellular targets, including endoplasmic reticulum, mitochondrial and plasma membranes, which contribute to further cell damage.

Zhu et al. (2010) pointed out that CCl₄ triggers cellular necrosis and apoptosis via the transformation of TNF- α and IL-1 β into proapoptotic factors that potentiate the apoptotic cascade from ROS- damaged mitochondria. Furthermore, CCl₄ interferes with calcium homeostasis. It promotes influx of calcium ions into the cytoplasm by physically disrupting membrane integrity via lipid peroxidation and by opening certain membrane calcium transport channels. It also inhibits active transport of calcium ions out of the cytoplasm (*Manibusan et al., 2007*). *Zowail et al. (2012)* added that calcium also could contribute to cell death by the over stimulation of calcium-responsive cellular enzymes that initiate a cascade of events, resulting in irreversible cell injury.

In mammals, there are two broad types of stem cells: embryonic stem cells, which are isolated from the inner cell mass of blastocyst, and adult stem cells, which are found in various tissues. There are three accessible sources of autologous adult stem cells in humans: Bone marrow, adipose tissue (lipid cells) and blood. Adult stem cells can also be taken from umbilical cord blood just after birth (*Scheers et al., 2011*). Light microscopic examination of stem cells displayed a typical fibroblast-like morphological features; stellate or branched star shaped, pale

basophilic cytoplasm and central oval nucleus with visible nucleoli (*Lennon and Caplan, 2006*).

Stem cell therapy is an intervention strategy that introduces new adult stem cells of damaged tissue in order to treat disease or injury. The ability of stem cells to self-renew and give rise to subsequent generations with variable degrees of differentiation capacities, offers significant potential for generation of tissues that can potentially replace diseased and damaged areas in the body, with minimal risk of rejection and side effects (*Gurtner et al., 2007*).

Stem cells express hepatocyte-like markers, which confer them a theoretical advantage for liver cell transplantation (*Karahuseyinoglu et al., 2007*). Rodents with liver damage was established using CCl₄ injection demonstrated reduced hepatic inflammation and extracellular matrix (ECM) deposition after MSCs transplantation. Mechanisms mediating these effects are thought to involve the modification of endogenous secreted factors i.e. metalloproteinases by MSCs (*Huang et al., 2009, Rabani et al., 2010 and Takami et al., 2014*).

The aim of the this study is to evaluate the possible therapeutic role of intravenous administration of mesenchymal stem cells against CCl₄-induced hepatotoxic changes.

2. Material and Methods:

Animals and experimental design:

Eighty adult male albino rats weighing 180-220 g were used in this study. They were obtained from the animal house, Faculty of Medicine, Cairo University. The rats were housed in separate cages and maintained under standard laboratory and environmental conditions with standard rat chow. The rats were divided into eight groups 10 rats each:

Group I (Normal control): The rats of this group received nothing and were sacrificed after 12 weeks.

Group II (Sham control): The rats of this group were injected intravenously once with one ml of isotonic saline and were sacrificed after 12 weeks.

Group III (CCl₄-induced hepatotoxicity for four weeks): The rats of this group were injected subcutaneously with CCl₄ twice weekly for four weeks and were sacrificed after the last injection.

Group IV (CCl₄-induced hepatotoxicity for four weeks followed by scarification after another four weeks): The rats of this group were injected subcutaneously with CCl₄ twice weekly for four weeks and were sacrificed after eight weeks.

Group V (CCl₄-induced hepatotoxicity for four weeks followed by MSC injection): The rats of this group were injected subcutaneously with CCl₄ twice weekly for four weeks followed by a single intravenous injection of MSC 24 hours after the last

dose of CCl₄. The rats were sacrificed after eight weeks.

Group VI (CCl₄-induced hepatotoxicity for eight weeks): The rats of this group were injected subcutaneously with CCl₄ twice weekly for eight weeks and were sacrificed after the last injection.

Group VII (CCl₄-induced hepatotoxicity for eight weeks followed by scarification after another four weeks): The rats of this group were injected subcutaneously with CCl₄ twice weekly for eight weeks and were sacrificed after 12 weeks.

Group VIII (CCl₄-induced hepatotoxicity for eight weeks followed by MSC injection): The rats of this group were injected subcutaneously with CCl₄ twice weekly for eight weeks followed by a single intravenous injection of MSC 24 hours after the last dose of CCl₄. The rats were sacrificed after 12 weeks.

At the end of each experimental period, blood sample from the tail vein of each rat was taken for biochemical study then rats were sacrificed by cervical dislocation

Chemicals:

CCl₄ was supplied from Sigma Aldrich as a solution mixed with olive oil 1:1 immediately before use. It was injected subcutaneously at a dose of 0.2 ml/kg body weight twice weekly for four weeks and eight weeks durations (*Chappell et al., 2016*).

Bone marrow (BM) - derived mesenchymal stem cells (MSC) were obtained from stem cell research unit at the Biochemistry Department of Kasr Al Aini, Faculty of Medicine, Cairo University. PKH26, red fluorescent cell linker mini kit for general cell membrane labeling (Sigma Aldrich, USA), Sigma brand, catalog number: MINI 26. It's in the form of PKH26 dye stock solution (1 vial containing 0.1 ml, 1x 10⁻³ M in ethanol) and diluent C (1 vial containing 10 ml). This dye has been used in groups V and VIII.

Stem cell dose: 1x10⁶ MSC labeled with PKH26 dye in 1 ml phosphate buffer saline (PBS) into the tail vein (*Levicar et al., 2008*).

Methods:

1- The liver was excised and processed for the following studies.

a- Light microscopic study using Hematoxylin and Eosin stain, Masson's trichrome stain and Periodic Acid Schiff reaction (PAS).

b- Electron microscopic study.

c- Fluorescence microscopic study to detect the mesenchymal stem cells.

2- Biochemical study: assessment of serum levels of liver enzymes Alanine Aminotransferase (ALT), Aspartate Aminotransferase (AST) and Gamma Glutamyl Transferase (GGT).

3- Histomorphometric study.

3. Results

Histological and ultrastructural results:

Group I (normal control group):

In the histological sections of the rat liver of the normal control group, stained with haematoxylin and eosin, the parenchyma showed uniform architecture. The hepatic lobules were seen consisting of intersecting plates of liver cells (hepatocytes) radiating outward from the central vein to the periphery of the lobule. Hepatic sinusoids were observed intervening between the hepatic plates, lined with flattened endothelial cells and the occasional deeply basophilic, stellate shaped Kupffer cells. The hepatocytes of this group appeared polyhedral in shape with granular acidophilic cytoplasm. Their nuclei were rounded in shape with well defined regular outline, binucleated hepatocytes were frequently encountered (**Fig.1**). The portal triad in the normal control rat liver section was seen formed of bile ductule lined with cuboidal or low columnar epithelium, a branch of the portal vein exhibiting a thin wall and wide lumen and branches of the hepatic artery characterized by a thicker wall and narrower lumen (**Fig.2**). In sections of rat liver of the normal control group, stained with PAS, the hepatocytes were shown to have a strong positive PAS reaction in the form of small red granules filling their cytoplasm denoting considerable amount of glycogen (**Fig.3**). Sections of the normal control rat liver, stained with Masson's trichrome visualized a normal pattern of collagen deposition-a thin layer of collagen fibers around the central vein and adjoining hepatic sinusoids and a small amount of collagen tissue in which the elements of the portal triad were located (**Figs.4, 5**). Examination of semithin sections revealed normal hepatic sinusoids and polyhedral hepatocytes with rounded nuclei having prominent nucleoli (**Fig.6**).

Electron microscopic examination of sections of rat liver of the normal control group revealed polyhedral hepatocytes with intervening adjoining hepatic sinusoids. The hepatocytes had an intact plasma membrane and abundant cytoplasmic organelles; spherical to ovoid mitochondria with intact cristae, parallel cisternae of rough endoplasmic reticulum covered by ribosomes and electron dense lysosomes. The nucleus was surrounded by a well defined nuclear envelope with nuclear pores and displayed evident nucleoli and dispersed chromatin with intact Golgi apparatus opposite these pores (**Fig.7**).

Group II (Sham control group): Specimens of rat liver of the sham control group, examined both by light and electron microscope revealed features similar to those observed in the normal control group.

Group III (CCl₄-induced hepatotoxicity for four weeks):

Histological liver sections of rats injected subcutaneously with CCl₄ twice weekly for 4 weeks, stained with haematoxylin and eosin showed moderately disturbed hepatic parenchymal architecture with inflammatory cellular infiltration around the central vein that was moderately congested and the elements of portal tract that exhibited moderately congested portal vein. The hepatic sinusoids also appeared congested or moderately dilated with moderate increase of Kupffer cells. The hepatocytes in the pericentral area (zone 3) and in the midzonal area (2) revealed vacuolated cytoplasm. Some nuclei demonstrated pyknotic like changes and some of them appeared karyolytic (**Figs. 8, 9**). Specimens stained with PAS displayed moderate positive PAS reaction denoting moderate glycogen content (**Fig. 10**).

Applying Masson's trichrome technique visualized moderate increase in collagen tissue deposition around the central vein, hepatic sinusoids and the elements of portal tract (**Figs.11, 12**). Examination of semithin sections revealed congested hepatic sinusoids. Most of hepatocytes exhibit nuclear pyknosis and karyolysis with indentation of nuclear envelope (**Fig.13**).

Electron microscopic examination of rat liver from the same group revealed congested hepatic sinusoid with Kupffer cells on its wall, thickened disrupted plasma membrane, the cytoplasm exhibited scattered areas of rarefaction and electron dense lysosomes. In some specimens, the mitochondria appeared normal but in other specimens they appeared ballooned with damaged cristae. The rough endoplasmic reticulum was swollen and fragmented, they had partially lost their ribosomal surface. Some nuclei showed clumps of chromatin material and blebbing of nuclear envelope (**Figs.14: a,14: b**).

Group IV (CCl₄-induced hepatotoxicity for four weeks followed by scarification after another four weeks):

Histological examination of liver sections of rats injected subcutaneously with CCl₄ twice weekly for four weeks and left for spontaneous recovery for one month revealed apparently preserved hepatic parenchymal architecture in some specimens and disturbed in others with inflammatory cellular infiltration in the portal area. However, there was mild to moderate congestion of the central vein and hepatic sinusoids with mild increase in Kupffer cells. Some hepatocytes showed mild vacuolation of their cytoplasm. Some pyknotic and karyolytic nuclei were observed (**Figs.15,16**).

In PAS stained sections, the hepatocytes revealed moderate glycogen content evidenced by a moderate PAS positive reaction (**Fig.17**). Using Masson's trichrome stain technique to visualize the deposition of collagen fibers showed mild increase around the

central vein, hepatic sinusoids as well as the portal areas (**Figs.18, 19**). Examination of semithin sections revealed congested hepatic sinusoids with Von Kupffer cells in their walls. Some hepatocytes exhibit nuclear pyknosis and karyolysis, few cells display apparently normal nuclei with prominent nucleoli. Mononuclear cellular infiltration can be observed (**Fig.20**).

Electron microscopic examination of some specimens of the rat liver of this group showed thick plasma membrane and electron dense lysosomes. Some hepatocytes exhibited moderate cytoplasmic rarefaction. Some nuclei presented clumps of chromatin material. Some mitochondria were ballooned and others had been apparently normal, rough endoplasmic reticulum were either fragmented and some of them are apparently normal with intact ribosomal surface and parallel cisterns (**Fig. 21**).

Group V (CCl₄-induced hepatotoxicity for four weeks followed by MSC injection):

MSCs labeled with PKH26 fluorescent dye detected in the hepatic tissue, confirmed homing of these cells into the liver tissue (**Fig.22**). Histological sections of the rat liver of this group revealed an apparently normal hepatic parenchymal architecture. The central vein was neither dilated nor congested. The hepatic sinusoids also appeared normal (**Fig.23**). The hepatocytes in all three zones were mostly normal with regular rounded nuclei, apart from few hepatocytes in the pericentral area of the hepatic lobule which exhibited minimal cytoplasmic vacuolation. The portal tract presented apparently normal features (**Figs.23, 24**). In histological sections of the rat liver of this group stained with PAS, most of the hepatocytes revealed high glycogen content as demonstrated by their strong positive PAS reaction (**Fig.25**). In Masson's trichrome stained sections, there was only minimal increase in the collagen fibers deposition around the central vein, hepatic sinusoids or in the portal tract (**Figs.26, 27**). Examination of semithin sections revealed mild congestion of hepatic sinusoids. Most of hepatocytes nuclei are apparently normal with prominent nucleoli. Few hepatocytes exhibit nuclear pyknosis and karyolysis (**Fig.28**).

Electron microscopic examination of the rat liver specimens of this group showed apparently normal hepatocytes with intact plasma membrane and rough endoplasmic reticulum that had been evenly distributed throughout the cytoplasm. The nuclei appeared normal with dispersed chromatin and intact nuclear envelope. Most of mitochondria appeared normal but few had been swollen with damaged cristae. Von Kupffer cell had been observed inside a non-congested hepatic sinusoid (**Fig. 29**).

Group VI (CCl₄-induced hepatotoxicity for eight weeks):

Histological examination of rat liver sections of rats injected subcutaneously with CCl₄ twice weekly for 8 weeks revealed disrupted hepatic parenchymal architecture in all specimens. The central vein was markedly dilated and congested. The hepatic sinusoids were also markedly dilated and congested especially in the pericentral area where severe extravasation of blood (haemorrhage) was also encountered. Marked increase in Kupffer cells and areas of hyaline degeneration have been observed as well (Fig.30).

The hepatocytes in all specimens displayed extensive pathologic changes, more evident in the pericentral area. The cells were swollen and their cytoplasm presented variable degrees of vacuolations and fatty degeneration. In all zones of the hepatic acini, the nuclei of the severely affected hepatocytes showed marked degenerative changes in the form of pyknosis and karyolysis (ghost forms). There was extensive inflammatory cellular infiltration in the portal area and the portal vein was severely congested. A markedly thickened wall of hepatic artery could be observed (Figs.30, 31, 32). In specimens stained with PAS, the hepatocytes showed faint PAS reaction indicating reduced glycogen content (Fig. 33). Using Masson's trichrome stain technique to visualize the deposition of collagen fibers showed a marked increase around the central vein, hepatic sinusoids as well as the portal areas (Figs.34,35).

Examination of semithin sections revealed marked congestion of hepatic sinusoids. Hepatocytes display extensive nuclear damage in the form of pyknosis and karyolysis (Fig. 36).

Electron microscopic study of rat liver specimens of this group showed marked ultrastructural changes in the hepatocytes; electron dense lysosomes, thick disrupted plasma membrane and the affected hepatocytes markedly swollen with fatty degeneration and extensive cytoplasmic vacuolation and rarefaction suggestive of hydropic degeneration- a characteristic feature of cellular damage. The nuclei in the majority of hepatocytes presented pyknosis, degenerated and marginated chromatin with blebbing of nuclear envelope (indented). The mitochondria showed variability in size and shape, enlargement (ballooning) with complete loss of their cristae and accumulated electron dense particles inside them. The rough endoplasmic reticulum appeared markedly degenerated forming aggregates near the nucleus in some hepatocytes or fragments that had lost their surface ribosomes in others and dilated congested hepatic sinusoid (Figs.37, 38).

Group VII (CCl₄-induced hepatotoxicity for eight weeks followed by scarification after another four weeks):

Histological examination of liver sections of rats injected subcutaneously with CCl₄ twice weekly for 8 weeks and left for spontaneous recovery for one month revealed moderately disturbed hepatic parenchymal architecture with marked inflammatory cellular infiltration in the portal area and around markedly congested and dilated central vein that was surrounded by hyaline degeneration. Furthermore, the hepatic sinusoids in the pericentral and midzonal areas showed marked dilatation. Most of hepatocytes in the pericentral and midzonal areas showed moderate cytoplasm vacuolation, nuclear pyknosis and karyolysis with marked increase in number of binucleated hepatocytes (Figs. 39, 40, 41). In specimens stained with PAS, the hepatocytes showed faint PAS reaction indicating reduced glycogen content (Fig.42). Using Masson's trichrome stain technique to visualize the deposition of collagen fibers showed a marked increase around the central vein, hepatic sinusoids as well as the portal areas (Figs. 43, 44). Examination of semithin sections revealed moderate congestion of hepatic sinusoids. Few hepatocytes display apparently normal nuclei with prominent nucleoli. Most of them show nuclear pyknosis and karyolysis (Fig.45).

Electron microscopic examination of most specimens of the rat liver of this group showed congested hepatic sinusoid, intact hepatocytes plasma membrane, scattered areas of cytoplasmic rarefaction and fatty degeneration. Some of mitochondria appeared normal and some of them had been markedly dilated (ballooning) with damaged cristae. Some of rough endoplasmic reticulum appeared markedly degenerated forming aggregates near the nucleus or fragments that lost their surface ribosomes, and some had been apparently normal with parallel cisterns. The nucleus displayed blebbing of nuclear membrane and peripheral condensation of chromatin material (Fig.46).

Group VIII (CCl₄-induced hepatotoxicity for eight weeks followed by MSC injection):

MSCs labeled with PKH26 fluorescent dye detected in the hepatic tissue, confirmed homing of these cells into the liver tissue (Fig.47). Histological examination of liver sections of rats injected subcutaneously with CCl₄ twice weekly for 8 weeks followed by single intravenous dose of MSC revealed preservation of normal hepatic parenchymal architecture with moderate increase in Von Kupffer cells. However, there was marked congestion and dilatation of the central vein and hepatic sinusoids. Some hepatocytes were binucleated. Several hepatocytes in the two above mentioned areas showed vacuolation of their cytoplasm. Some hepatocytes had nuclei that displayed pyknosis and karyolysis (Fig.48). The portal area showed moderately dilated congested

portal vein, moderately thick-walled hepatic artery with mild mononuclear cellular infiltration. Some hepatocytes revealed cytoplasmic vacuolation, pyknotic and karyolytic nuclei (**Fig. 49**). In PAS stained sections, the hepatocytes revealed moderate glycogen content evidenced by a moderate PAS reaction (**Fig.50**). Using Masson's trichrome stain technique to visualize the deposition of collagen fibers showed a moderate increase around the central vein, hepatic sinusoids as well as the portal areas (**Figs.51, 52**). Examination of semithin sections revealed moderate congestion of hepatic sinusoids. Some hepatocytes display apparently normal nuclei with prominent nucleoli. Some of them show nuclear pyknosis and karyolysis (**Fig.53**).

Electron microscopic examination of specimens of the rat liver of this group showed preserved hepatocytes plasma membrane, few areas of cytoplasmic rarefaction and fatty degeneration. The mitochondria had been apparently normal with their cristae. The rough endoplasmic reticulum appeared normal with parallel cistern and their ribosomal surface. The nucleus appeared normal in some specimens with intact nuclear envelope and prominent nucleoli, and displayed few clumps of chromatin material with slightly indented (blebbing) nuclear envelope in others (**Fig.54**).

Results of histomorphometric study:

Statistical study of liver enzymes levels:

Further to the architectural disturbance, there was functional impairment manifested as an increase in liver enzymes concentration in groups injected with CCl₄. The levels of liver enzymes ALT, AST and GGT showed no statistically significant increase or decrease between group I and group II (**table 1**) and between group I and group V (**table 3**) with p-value (>0.05). However, there was statistically significant increase with p-value (<0.05) between group I and group VIII with high mean among group VIII (**table 5**). There was significant difference with p-value (<0.05) between group V and group VIII as regards to liver enzymes with high mean among group VIII (**table 7**).

In CCl₄ administration groups for four weeks, there was statistically significant increase with p-value (<0.05) between group III and group IV as regards to AST and GGT liver enzymes with high mean among group III. On the other hand there was no statistically

significant difference with p-value (>0.05) as regards to ALT level (**table 9**). However, there was statistically significant decrease with p-value (<0.05) between group III and group V as regards to ALT, AST and GGT liver enzymes with high mean among group III (**table 11**). In comparison between III and VI study groups regarding level of liver enzymes, there was statistically significant decrease with p-value (<0.05) between both groups with high mean among group VI (**table 13**) and between group IV and group VII with high mean among group VII (**table 15**).

In CCl₄ administration groups for eight weeks, there was no statistically significant difference with p-value (>0.05) between group VI and group VII as regards to AST, ALT and GGT liver enzymes (**table 17**). On the other hand, there was statistically significant increase with p-value (<0.05) between group VI and group VIII as regards to AST, ALT and GGT liver enzymes with high mean among group VI (**table 19**).

Statistical study of degree of liver fibrosis:

The degree of liver fibrosis showed no statistically significant increase or decrease between group I and group II (**table 2**) and between group I and group V (**table 4**) with p-value (>0.05). However, there was statistically significant difference with p-value (<0.05) between group I and group VIII as regards to degree of liver fibrosis with high mean among group VIII (**table 6**). There was statistically significant difference with p-value (<0.05) between group V and group VIII as regards to degree of liver fibrosis with high mean among group VIII (**table 8**). In CCl₄ administration groups for four weeks, There was no statistically significant difference with p-value (>0.05) between group III and group IV (**table 10**). There was statistically significant difference with p-value (<0.05) between group III and group V (**table 12**) and between group III and group VI as regards to degree of liver fibrosis (**table 14**). In CCl₄ administration groups for eight weeks, there was statistically significant decrease with p-value (<0.05) between group IV group VII as regards to degree of liver fibrosis with high mean among group VII (**table 16**). There was no statistically significant difference with p-value (>0.05) between group VI and group VII (**table 18**) and between group VI and group VIII with p-value (>0.05) (**table 20**).

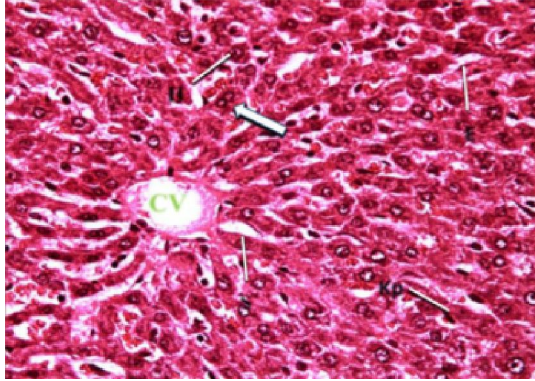


Fig. (1): Micrograph of group I (*Normal control*) showing normal hepatic architecture- hepatocytes (H) radiating from the central vein (CV) and hepatic sinusoids (S) lined with flattened endothelial cells (E) and Von Kupffer cells (kp). Binucleated hepatocytes are also seen (arrow). (Hx. & E. X400)

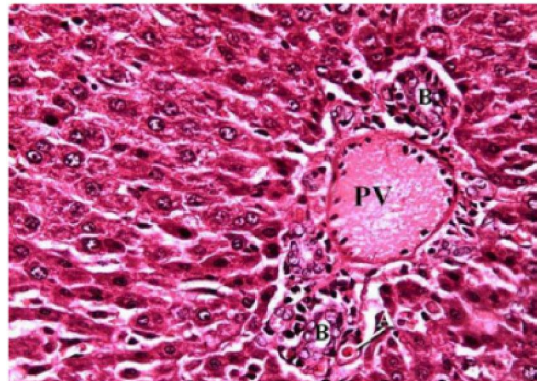


Fig. (2): Micrograph of group I showing the portal triad: bile ductile (B), portal vein (PV) and hepaticartery (A).(Hx. & E. X400)

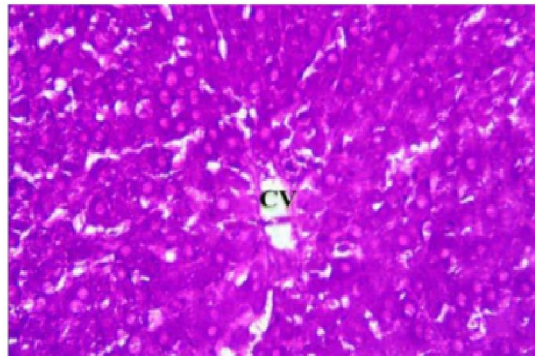


Fig. (3): Micrograph of group I exhibiting a strong positive PAS reaction of the hepatocytic plates radiating from the central vein (CV). (PAS; X400)

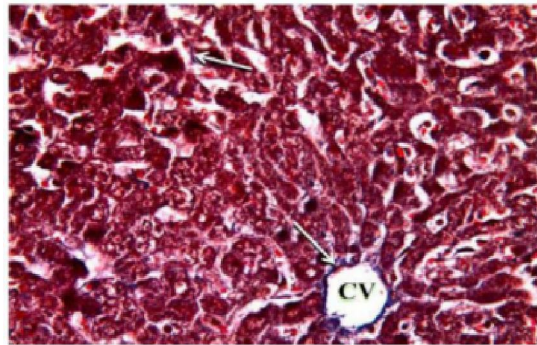


Fig. (4): Micrograph of group I showing the normal distribution of collagen bundles (arrows) around the central vein (CV) and hepatic sinusoids.(Masson's trichrome; X400)

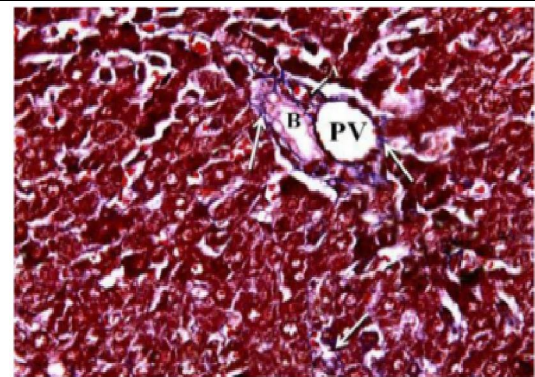


Fig. (5): Micrograph of group I, showing the normal distribution of collagen bundles (arrows) around the components of the portal triad: bile ductile (B), portal vein (PV) and adjoining hepatic sinusoids. (Masson's trichrome; X400).

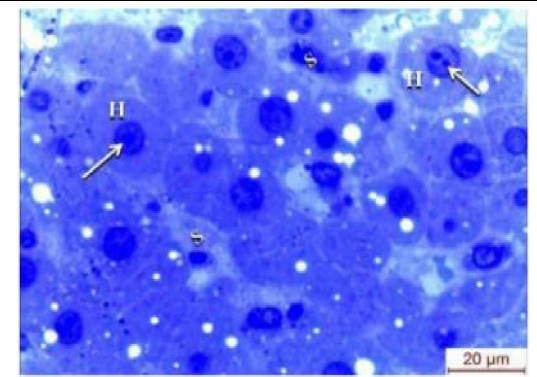


Figure (6): Micrograph of group I showing normal hepatocytes (H) with prominent nucleoli (arrows) and hepatic sinusoids (S). (Toluidine blue x 1000).

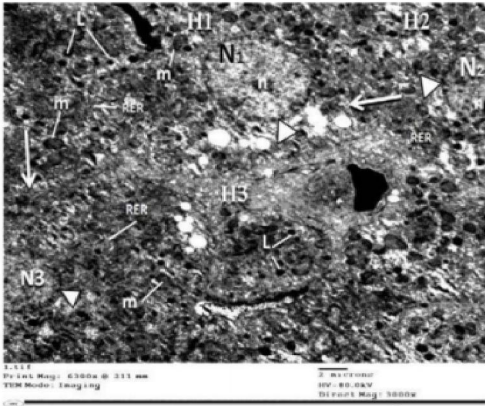


Fig. (7): Ultragraph of group I displaying hepatic sinusoid (S) between polyhyal hepatocytes (H1, H2, H3) that exhibit intact plasma membrane (arrow), abundant mitochondria (m) and rough endoplasmic reticulum (RER), electron dense lysosomes (L). The nucleus (N1, N2, N3) is surrounded by an envelope (arrowhead) and display dispersed chromatin and evident nucleoli (n). (EM; X 3000).

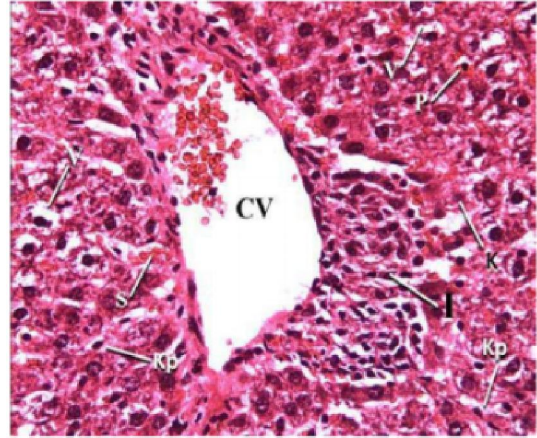


Fig. (8): Micrograph of group III of the liver showing disturbed parenchymal architecture. The central vein (CV) is engorged and dilated. Hepatic sinusoids (S) appeared engorged. Hepatocytes exhibit cytoplasmic vacuolation (V), pyknotic nuclei (P) and karyolysis (K). Mononuclear cell infiltration (I) and increased Von Kupffer cells (kp) can be observed. (Hx. & E. X400)

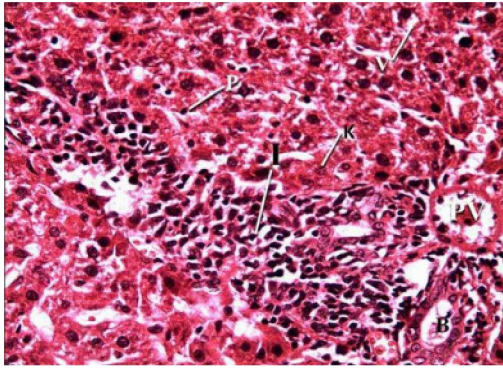


Fig. (9): Micrograph of group III showing mononuclear cell infiltration (I) around bile ductules (B) and engorged portal vein (PV). Hepatocytes exhibit cytoplasmic vacuolation (V), nuclear pyknosis (P) and karyolysis (K). (Hx. & E. X400)

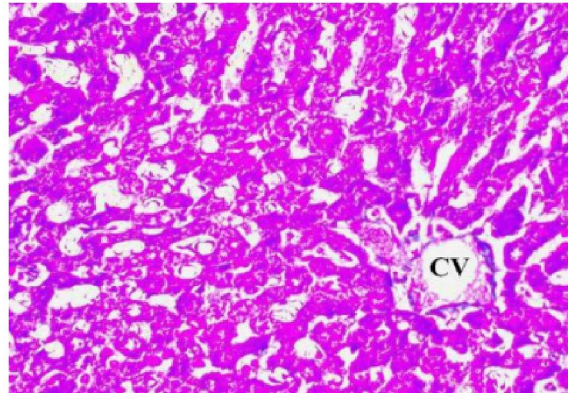


Fig. (10): Micrograph of group III presenting moderate positive PAS reaction denoting moderate glycogen content in the hepatocytes radiating from the central vein (CV). (PAS; X400).

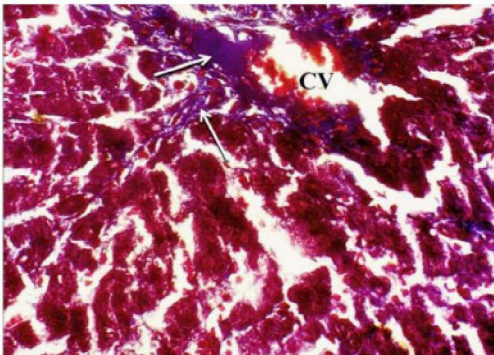


Fig. (11): Micrograph of group III showing moderate increase of collagen bundles (arrows) around the central vein (CV) and hepatic sinusoids. (Masson's trichrome; X400).

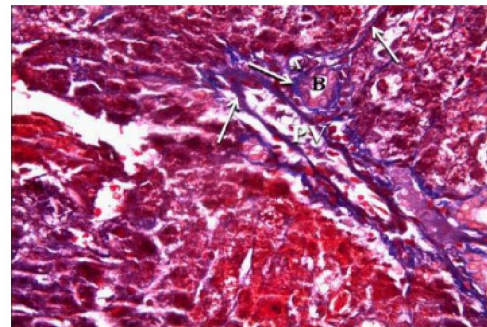


Fig. (12): Micrograph of group III displaying moderately increased collagen fibers deposition (arrows) around the portal triad: bile ductile (B), portal vein (PV), hepatic arteriole (A) and hepatic sinusoids. (Masson's trichrome; X400)

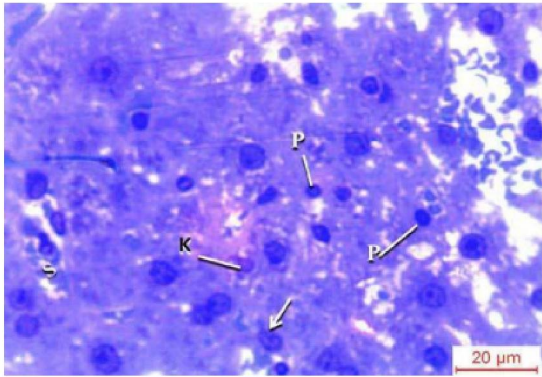


Figure (13): Micrograph of group III showing congested hepatic sinusoids (S). Most of hepatocytes exhibit nuclear pyknosis (P) and karyolysis (K) with indentation of nuclear envelope (arrow). (Toluidine blue x 1000)

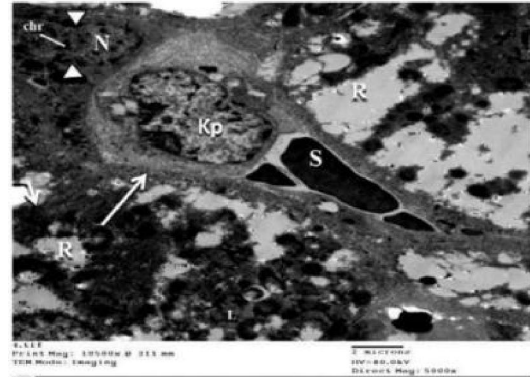


Fig. (14: a): Ultragraph of group III displaying Von Kupffer cell (Kp) inside a congested hepatic sinusoid (S). The hepatocyte exhibits thick (arrow) denuded (short arrow) plasma membrane, cytoplasmic rarefaction (R), electron dense lysosomes (L). The nucleus (N) shows chromatin clumps (chr) and blebbing (arrowhead) of nuclear envelope. (EM; X 5000)

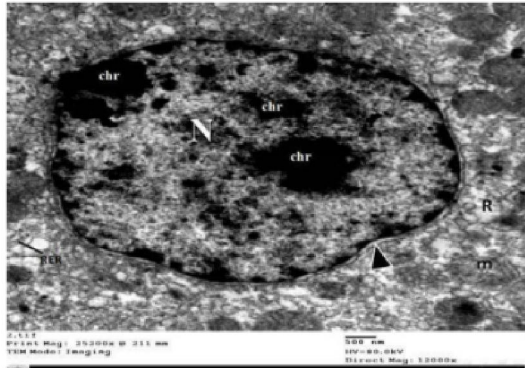


Fig. (14: b): Ultragraph of group III displaying cytoplasmic rarefaction (R), ballooning of mitochondria with lost crista (m) and fragmented rough endoplasmic reticulum forming cisterns and partially lost ribosomal surface (RER). The nucleus (N) shows chromatin clumps (chr) and blebbing (arrowhead) of nuclear envelope. (EM; X 12000)

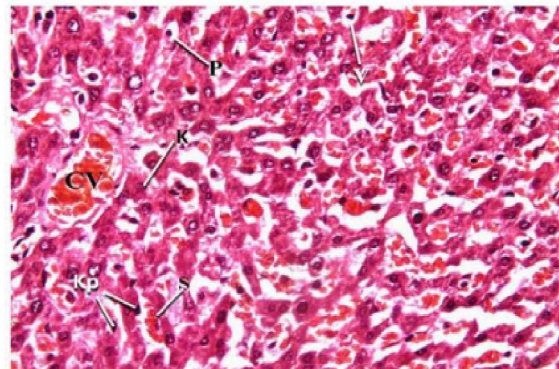


Fig. (15): Micrograph of group IV showing disturbed parenchymal architecture and increased Von Kupffer cells (kp). Engorged central vein (CV) and hepatic sinusoids (S). Some hepatocytes exhibit cytoplasmic vacuolation (V), nuclear pyknosis (P) and karyolysis (K). (Hx. & E. X400)

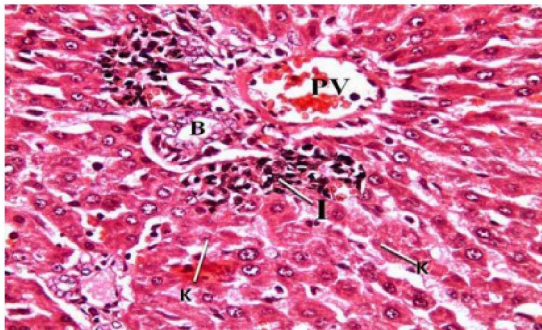


Fig. (16): Micrograph of group IV showing mild mononuclear cell infiltration (I) around bile ductules (B) and engorged portal vein (PV). Nuclei of some hepatocytes exhibit karyolysis (K). (Hx. & E. X400)

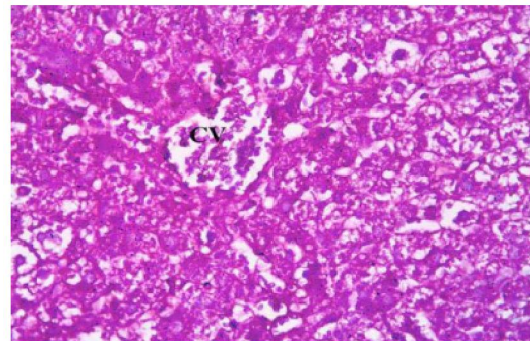


Fig. (17): Micrograph of group IV presenting moderate positive PAS reaction denoting moderate glycogen content in the hepatocytes radiating from the central vein (CV). (PAS; X400)

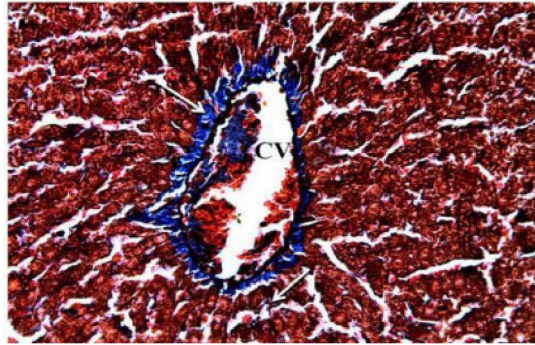


Fig. (18): Micrograph of group IV showing mild increase of collagen bundles (arrows) around the central vein (CV) and hepatic sinusoids. (Masson's trichrome; X400)

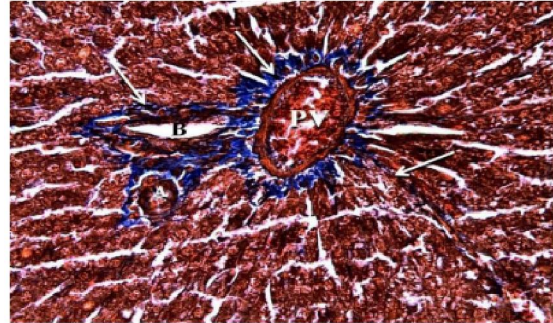


Fig. (19): Micrograph of group IV displaying mild increase of collagen bundles (arrows) around the portal triad: bile ductile (B), portal vein (PV), hepatic arteriole (A) and adjoining hepatic sinusoids. (Masson's trichrome; X400)

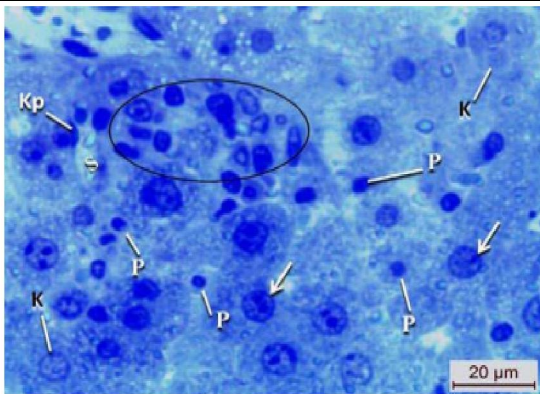


Figure (20): Micrograph of group IV showing congested hepatic sinusoids (S) with Von Kupffer cells (kp) in their walls. Some hepatocytes exhibit nuclear pyknosis (P) and karyolysis (K), few cells display apparently normal nuclei with prominent nucleoli (arrows). Mononuclear cellular infiltration can be observed (circle). (Toluidine blue x 1000)

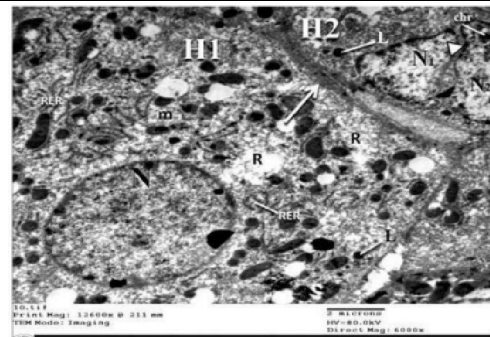


Fig. (21): Ultragraph of group IV displaying thick plasma membrane (arrow), between two hepatocytes (H1, H2). H1 shows cytoplasmic rarefaction (R), ballooning of mitochondria (m) with lost cristae, fragmented rough endoplasmic reticulum (RER) forming cisterns and apparently normal nucleus (N), while the binucleated (H2) exhibits a karyolytic nucleus (N1) and another nucleus (N2) with chromatin clumps (chr) and blebbing of nuclear envelope (arrowhead). Both (H1) and (H2) display electron dense lysosomes (L) (EM; X 6000).

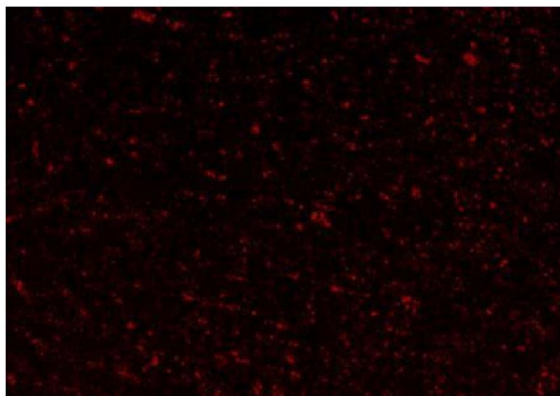


Fig. (22): labeling of MSCs with PKH26 dye.

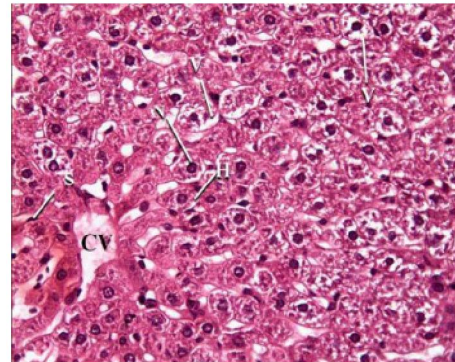


Fig. (23): Micrograph of group V showing apparently normal parenchymal architecture. Most hepatocytes (H) are apparently normal and display regular rounded nuclei (N) few hepatocytes exhibit cytoplasmic vacuolation (V). Hepatic sinusoids (S) are seen radiating from the central vein (CV). (Hx. & E. X400)

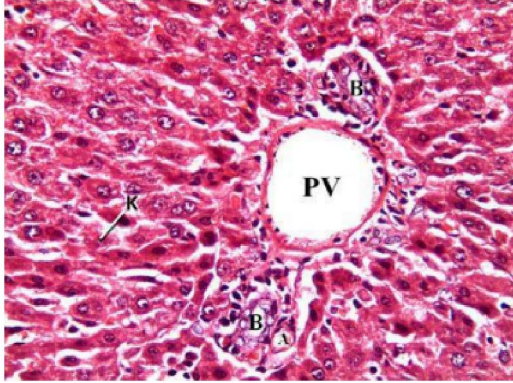


Fig. (24): Micrograph of group V showing apparently normal portal triad: the portal vein (PV), bile duct (B) and hepatic artery (A). Nuclei of few hepatocytes appeared karyolytic (k). (Hx. & E. X400)

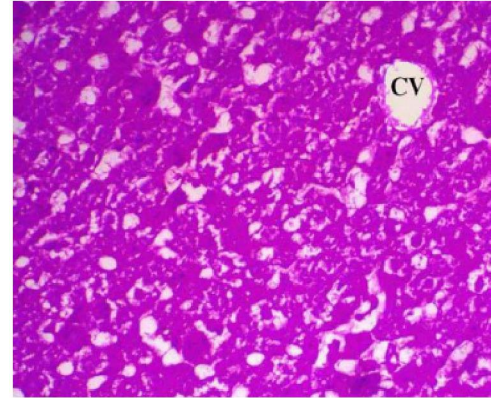


Fig. (25): Micrograph of group V exhibiting a strong positive PAS reaction of the hepatocytic plates radiating from the central vein (CV). (PAS; X400)

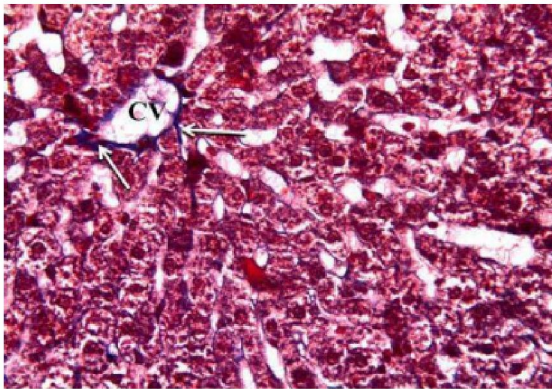


Fig. (26): Micrograph of group V displaying minimal increase in collagen bundles (arrows) around the central vein (CV) and adjoining hepatic sinusoids. (Masson's trichrome; X400)

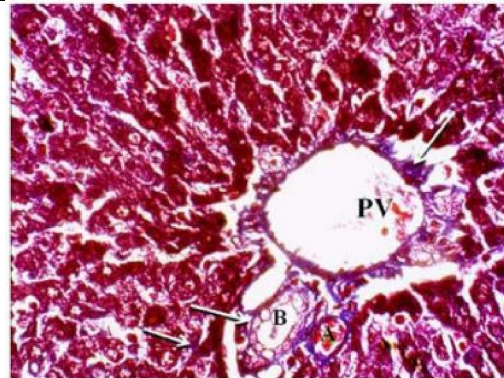


Fig. (27): Micrograph of group V showing minimal increase in collagen bundles (arrows) around the portal triad: bile duct (B), portal vein (PV), hepatic arteriole (A) and adjoining hepatic sinusoids. (Masson's trichrome; X400)

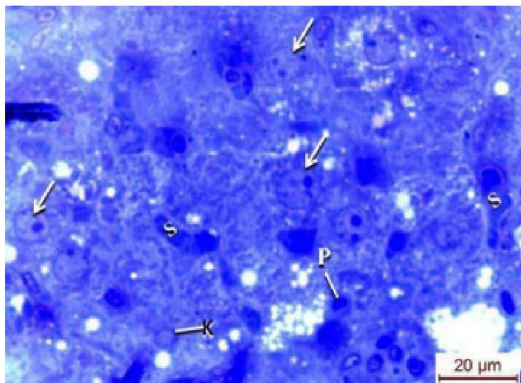


Figure (28): Micrograph of group V showing mild congestion of hepatic sinusoids (S). Most of hepatocytes nuclei are apparently normal with prominent nucleoli (arrows). Few hepatocytes exhibit nuclear pyknosis (P) and karyolysis (K). (Toluidine blue x 1000)

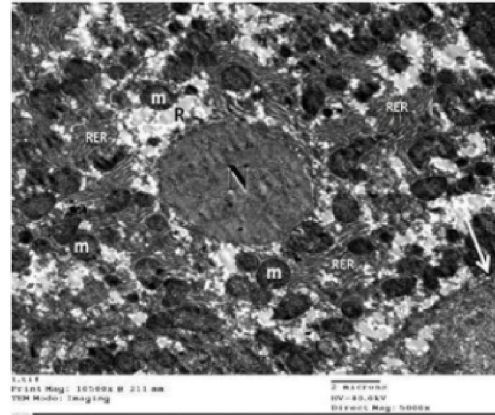


Fig. (29): Ultragraph of group V displaying apparently normal nucleus (N) with dispersed chromatin, an intact plasma membrane (arrow), abundant mitochondria (m) with normal cristal pattern, intact rough endoplasmic reticulum with parallel cisterns (RER) and cytoplasmic rarefaction (R). (EM; X 5000).

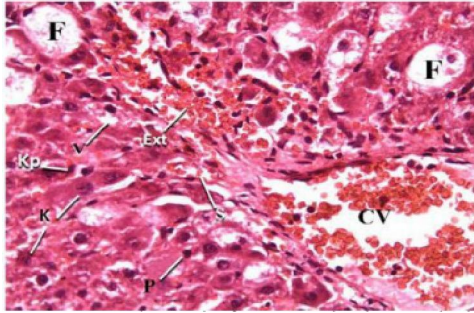


Fig. (30): Micrograph of group VI showing completely disturbed hepatic parenchymal architecture, marked increased in Von Kupffer cells (**kp**), markedly congested central vein (**CV**) and hepatic sinusoids (**S**). Most hepatocytes exhibit extensive cytoplasmic vacuolation (**V**), fat degeneration (**F**), nuclear pyknosis (**P**) and karyolysis (**K**). Extravasated blood (**Ext**) can be seen. (**Hx. & E. X400**)

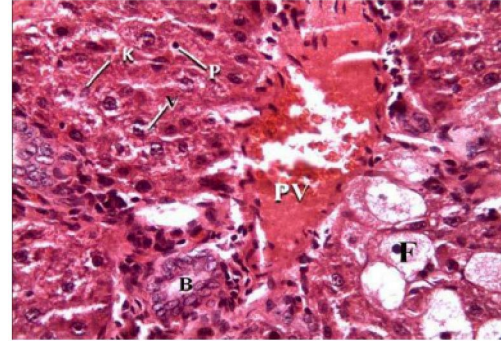


Fig. (31): Micrograph of group VI showing markedly congested portal vein (**PV**). Hepatocytes are swollen and exhibit fat degeneration (**F**), cytoplasmic vacuolation (**V**), pyknotic (**P**) and karyolytic nuclei (**K**). (**Hx. & E. X400**)

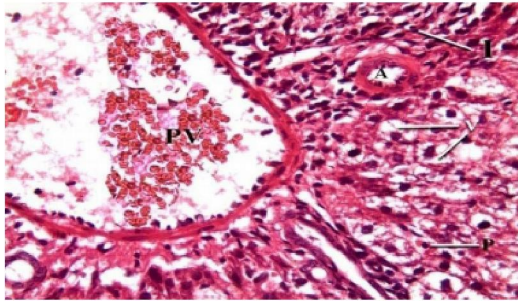


Fig. (32): Micrograph of group VI displaying markedly engorged portal vein (**PV**), marked thickened wall of hepatic artery (**A**) and marked inflammatory cellular infiltration (**I**). Hepatocytes exhibit extensive cytoplasmic vacuolation (**V**) and pyknotic (**P**) nuclei. (**Hx. & E. X400**)

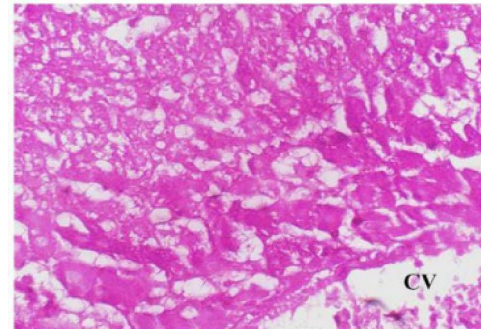


Fig. (33): Micrograph of group VI presenting faint PAS reaction of hepatocytes radiating from the central vein (**CV**). (**PAS; X400**)

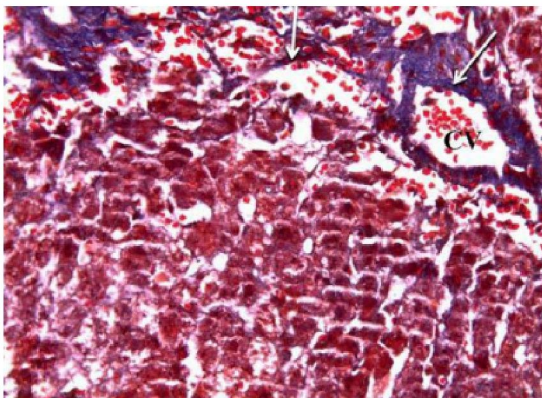


Fig. (34): Micrograph of group VI displaying marked increase in collagen bundles (**arrows**) around the central vein (**CV**) and adjoining hepatic sinusoids. (**Masson's trichrome; X400**)

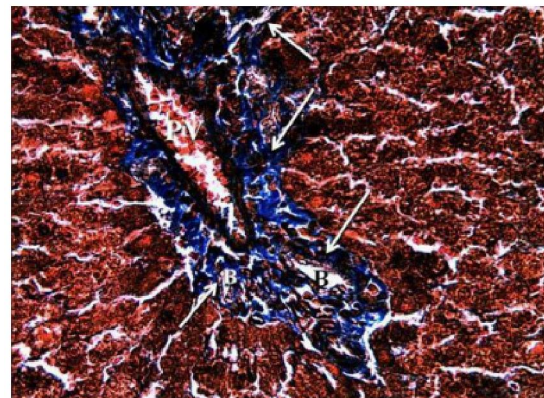


Fig. (35): Micrograph of group VI displaying extensively increased collagen bundles (**arrows**) around the portal triad: bile duct (**B**), portal vein (**PV**), hepatic arteriole (**A**) and adjoining hepatic sinusoids. (**Masson's trichrome; X400**)

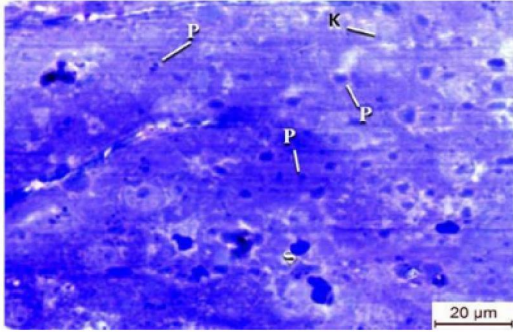


Figure (36): Micrograph of group VI showing marked congestion of hepatic sinusoids (S). Hepatocytes display extensive nuclear damage in the form of pyknosis (P) and karyolysis (K). (Toluidine blue x 1000)

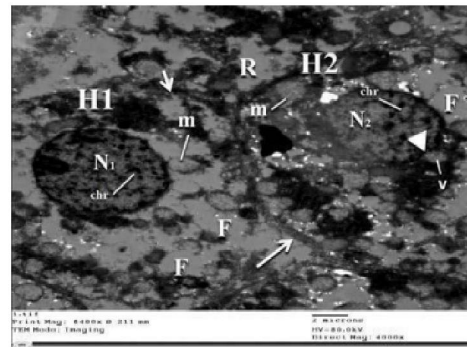


Fig. (37): Ultragraph of group VI displaying thick (arrow) denuded (short arrow) plasmamembrane between two hepatocytes (H1, H2) that display degeneration of cytoplasm in the form of vacuolation (V), rarefaction (R) and extensive fatty degeneration (F), ballooned mitochondria with damaged cristae (m). The nuclei of both hepatocytes (N1, N2) exhibit chromatin clumps (chr) with indentation (blebbing) of nuclear envelope (arrowhead) of (N2). (EM; X 4000)

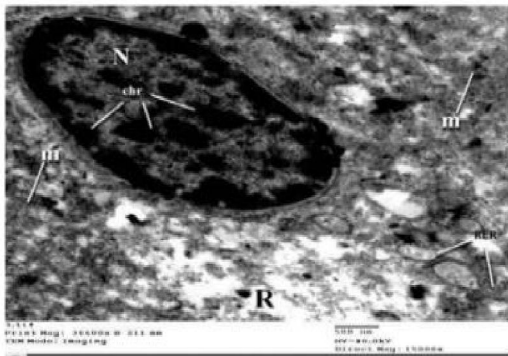


Fig. (38): Ultragraph of group VI displaying cytoplasmic rarefaction (R) ballooned mitochondria with damaged crista (m) and electron dense particles inside, fragmented largely dilated rough endoplasmic reticulum (RER). The nucleus exhibits chromatin clumps and peripheral margination of chromatin material (chr). (EM; X 15000)

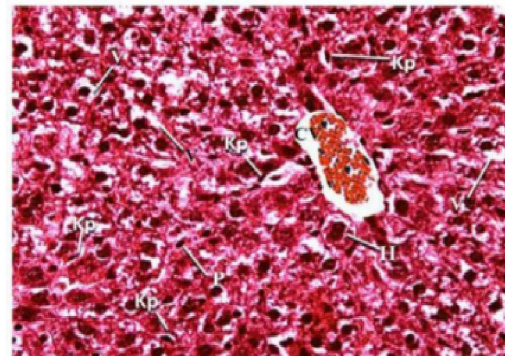


Fig. (39): Micrograph of group VII showing mildly disturbed hepatic parenchymal architecture, marked increase in Von Kupffer cells (kp) with moderately congested dilated central vein (CV). Most of hepatocytes (H) are binucleated and some of them are swollen. Extensive cytoplasmic vacuolation (V) and nuclear pyknosis (P) can be observed. (Hx. & E. X400)

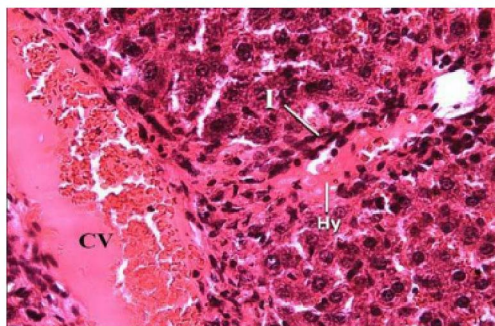


Fig. (40): Micrograph of group VII showing area of hyaline degeneration (Hy) and inflammatory cellular infiltration (I) around moderately congested dilated central vein (CV). (Hx. & E. X400)

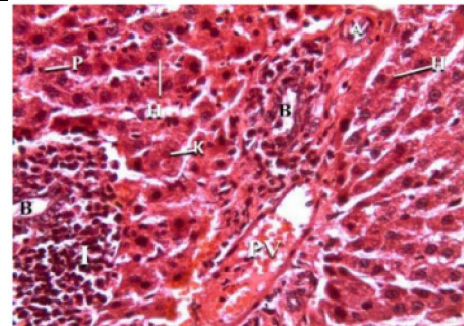


Fig. (41): Micrograph of group VII displaying moderately congested portal vein (PV), thick walled hepatic artery (A) and moderate mononuclear cell infiltration (I) around the bile ductules (B). Increased binucleated hepatocytes (H) and pyknotic (P) nuclei. (Hx. & E. X400)

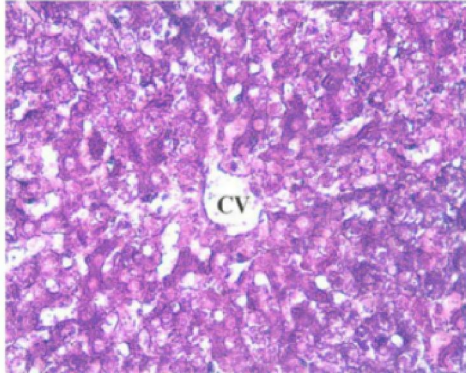


Fig. (42): Micrograph of group VII presenting faint positive PAS reaction of hepatocytes radiating from the central vein (CV). (PAS; X400)

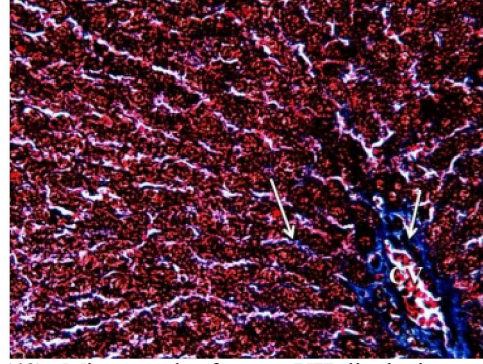


Fig. (43): Micrograph of group VII displaying marked increase in collagen fibers (arrows) deposition around the central vein (CV) and adjoining hepatic sinusoids. (Masson's trichrome; X400)

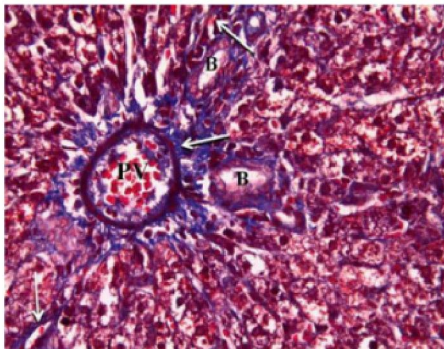


Fig. (44): Micrograph of group VII displaying markedly increased collagen bundles (arrows) around bile ductile (B) and portal vein (PV) and adjoining hepatic sinusoids. (Masson's trichrome; X400)

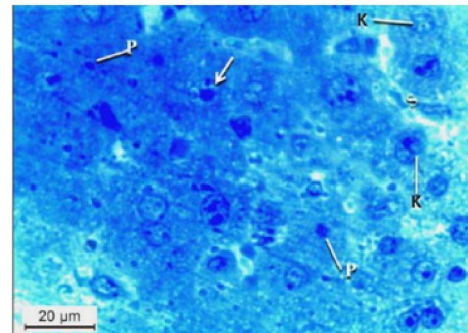


Figure (45): Micrograph of group VII showing moderate congestion of hepatic sinusoids (S). Few hepatocytes display apparently normal nuclei with prominent nucleoli (arrows). Most of them show nuclear pyknosis (P) and karyolysis (K). (Toluidine blue x 1000)



Fig. (46): Ultragraph of group VII displaying congested hepatic sinusoid (S) between hepatocytes (H1, H3) that display an intact plasma membrane (arrow). Hepatocytes (H1, H2, H3) exhibit either fatty degeneration (F) or cytoplasmic rarefaction (R), dilated rough endoplasmic reticulum (RER), most of mitochondria are apparently normal (m1) and few of them are ballooned with damaged cristae (m2). The nuclei (N1, N2) in (H1, H2) exhibit chromatin clumps and peripheral margination of chromatin material (chr) with blebbing of nuclear envelope (arrowhead). (EM; X 5000)

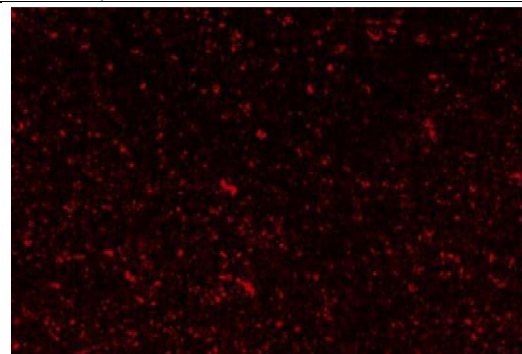


Fig. (47): labeling of MSCs with PKH26 dye.

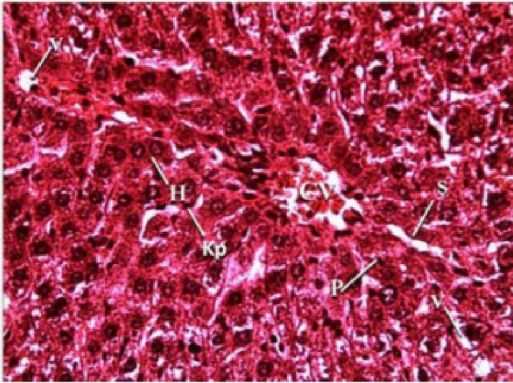


Fig. (48): Micrograph of group VIII showing apparently normal parenchymal architecture, moderate increase in Von Kupffer cells (kp) with marked congestion of central vein (CV). Some hepatocytes (H) are binucleated. Cytoplasmic vacuolation (V) and pyknotic nuclei (P) can be observed. (Hx. & E. X400)

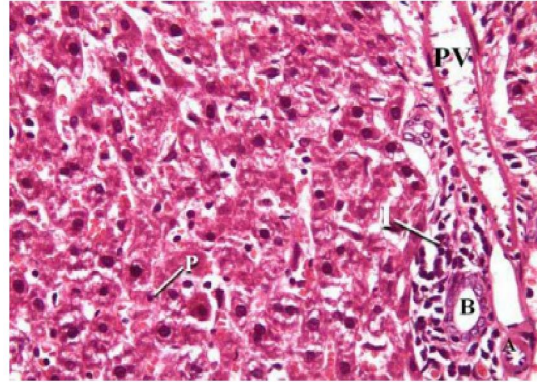


Fig. (49): Micrograph of group VIII displaying mildly engorged portal vein (PV), moderately thick walled hepatic artery (A) and mild mononuclear cell infiltration (I) around the bile ductules (B). Some hepatocytes (H) exhibit cytoplasmic vacuolation (V), nuclear pyknosis (P) and karyolysis (K). (Hx. & E. X400)

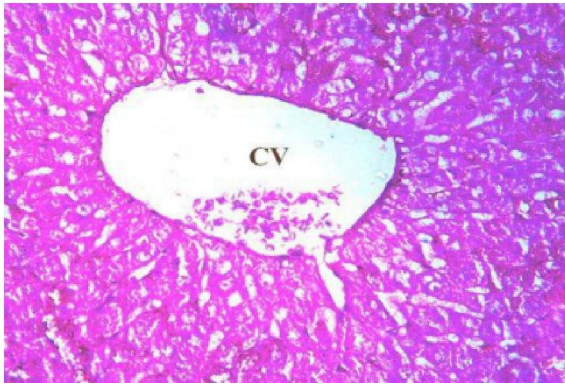


Fig. (50): Micrograph of group VIII presenting moderate positive PAS reaction denoting moderate glycogen content in the hepatocytes radiating from the central vein (CV). (PAS; X400)

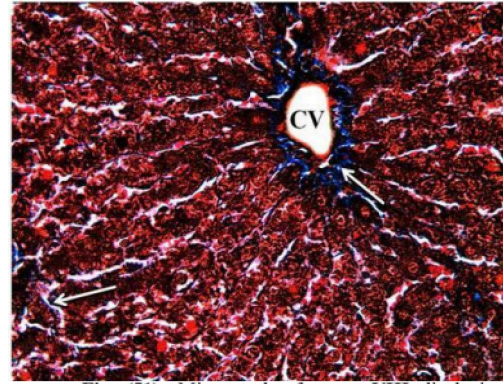


Fig. (51): Micrograph of group VIII displaying moderate increase in collagen bundles (arrows) around the central vein (CV) and adjoining hepatic sinusoids. (Masson's trichrome; X400)

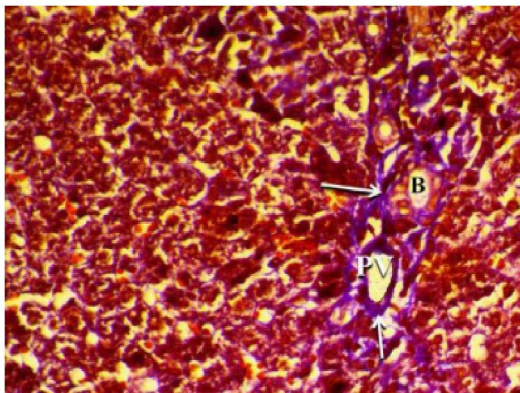


Fig. (52): Micrograph of group VIII displaying moderate increase in collagen bundles (arrows) around bile ductile (B), portal vein (PV) and adjoining hepatic sinusoids. (Masson's trichrome; X400)

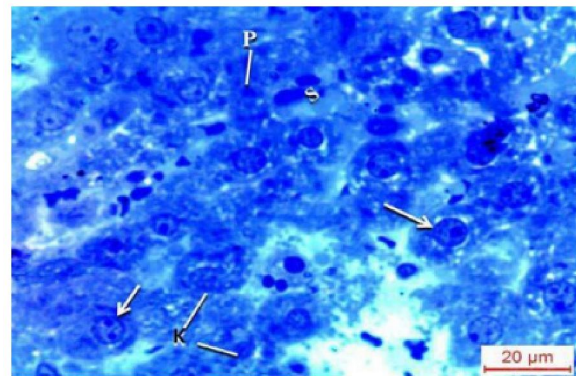


Figure (53): Micrograph of group VIII showing moderate congestion of hepatic sinusoids (S). Some hepatocytes display apparently normal nuclei with prominent nucleoli (arrows). Some of them show nuclear pyknosis (P) and karyolysis (K). (Toluidine blue x 1000)

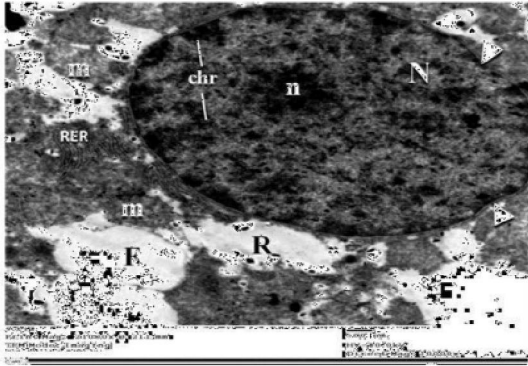


Fig. (54): Ultragraph of group VIII displaying apparently normal mitochondria (m) and roughendoplasmic reticulum (RER) with its ribosomal surface and scattered areas of cytoplasmic rarefaction (R) and fatty degeneration (F). The nucleus (N) appears normal with prominent nucleolus (n), fewchromatin clumbs (chr) and blebbing of nuclear envelope (arrowhead). (EM; X 10000)

Table (1): Comparison between I & II study groups regarding level of liver enzymes with p-value (>0.05).

Liver enzymes (U/ml)	Normal Control	Sham Control	p-value	Sig.
	Mean ± SD	Mean ± SD		
ALT	17.8±2	18.2±2	0.8	NS
AST	11.2±1.2	12.2±1.2	0.2	NS
GGT	21.2±0.8	20.1±2	0.5	NS

Table (2): Comparison between I & II study groups regarding degree of liver fibrosis with p-value (>0.05).

Collagen	Normal Control	Sham control	p-value	Sig.
	Mean ± SD	Mean ± SD		
Area	131321.3±39633.5	124642.1±42496.	0.8	NS
Area fract	0.042±0.013	0.042±0.018	0.9	NS
Area fill	0.046±0.018	0.042±0.016	0.7	NS
Area %	4.38±1.32	4.15±1.41	0.8	NS

Table (3): Comparison between I & V study groups regarding level of liver enzymes with p-value (>0.05).

Liver enzymes (u/ml)	Normal Control	CC14 (4 Ws) & MSC injection	p-value	Sig.
	Mean ± SD	Mean ± SD		
ALT	17.8±2	20.9±2.6	0.06	NS
AST	11.2±1.2	15.7±5.5	0.1	NS
GGT	21.2±0.8	25.7±4.3	0.07	NS

Table (4): Comparison between I, V study groups regarding degree of liver fibrosis, p-value (>0.05).

Collagen	Normal Control	CC14 (4 Ws) & MSC injection	p-value	Sig.
	Mean ± SD	Mean ± SD		
Area	131321.3±39633.5	168544.8±63974.5	0.3	NS
Area fract	0.042±0.013	0.056±0.021	0.3	NS
Area fill	0.046±0.018	0.06±0.026	0.4	NS
Area %	4.38±1.32	5.62±2.13	0.3	NS

Table (5): Comparison between I & VIII study groups regarding level of liver enzymes with p-value (<0.05).

Liver enzymes (u/ml)	Normal Control	CC14 (8 Ws) & MSC injection	p-value	Sig.
	Mean ± SD	Mean ± SD		
ALT	17.8±2	39.9±2.7	<0.001	HS
AST	11.2±1.2	29.6±6	0.001	HS
GGT	17.8±2.4	35.8±6.1	0.002	HS

Table (6): Comparison between I & VIII study groups regarding degree of liver fibrosis, p-value (<0.05).

Collagen	Normal Control	CC14 (8 Ws) & MSC injection	p-value	Sig.
	Mean ± SD	Mean ± SD		
Area	131321.3±39633.5	441257±41376.7	<0.001	HS
Area fract	0.042±0.013	0.15±0.014	<0.001	HS
Area fill	0.046±0.018	0.174±0.019	<0.001	HS
Area %	4.38±1.32	14.7±1.4	<0.001	HS

Table (7): Comparison between V & VIII study groups regarding level of liver enzymes. p-value (<0.05)

Liver enzymes	CC14 (4 Ws) & MSC injection	CC14 (8 Ws) & MSC injection	p-value	Sig.
	Mean ± SD	Mean ± SD		
ALT	20.9±2.6	39.9±2.7	<0.001	HS
AST	15.7±5.5	29.6±6	0.005	HS
GGT	25.7±4.3	35.8±6.1	0.02	S

Table (8): Comparison between V & VIII study groups regarding degree of liver fibrosis. p-value (<0.05)

collagen	CC14 (4 Ws) & MSC injection	CC14 (8 Ws) & MSC injection	p-value	Sig.
	Mean ± SD	Mean ± SD		
Area	168544.8±63974.5	441257±41376.7	<0.001	HS
Area fract	0.056±0.021	0.15±0.014	<0.001	HS
Area fill	0.060±0.026	0.174±0.019	<0.001	HS
Area %	5.62±2.13	14.7±1.4	<0.001	HS

Table (9): Comparison between III & IV study groups regarding level of liver enzymes. p-value (<0.05).

Liver enzymes (u/ml)	CC14 (4 Ws)	CC14 (4 Ws) & Scarification	p-value	Sig.
	Mean ± SD	Mean ± SD		
ALT	68.5±11.3	57.9±10.5	0.2	NS
AST	47.5±9.2	36.6±3.3	0.03	S
GGT	68.4±5.9	48.5±12.7	0.01	S

Table (10): Comparison between III & IV study groups regarding degree of liver fibrosis, p-value (>0.05).

Collagen	CC14 (4 Ws)	CC14 (4 Ws) & Scarification	P-value	Sig.
	Mean ± SD	Mean ± SD		
Area	371442.1±7169.4	283850.4±66930.7	0.08	NS
Area fract	0.13±0.024	0.094±0.023	0.06	NS
Area fill	0.142±0.033	0.108±0.027	0.1	NS
Area %	12.4±2.4	9.46±2.22	0.08	NS

Table (11): Comparison between III & V study groups regarding level of liver enzymes. p-value (<0.05)

Liver enzymes (u/ml)	CC14 (4 Ws)	CC14 (4 Ws) & MSC injection	p-value	Sig.
	Mean ± SD	Mean ± SD		
ALT	68.5±11.3	20.9±5.6	<0.001	HS
AST	47.5±9.2	15.7±5.5	<0.001	HS
GGT	68.4±5.9	25.7±4.3	<0.001	HS

Table (12): Comparison between III & V study groups regarding degree of liver fibrosis, p-value (<0.05).

Collagen	CC14 (4 Ws)	CC14 (4 Ws) & MSC injection	p-value	Sig.
	Mean ± SD	Mean ± SD		
Area	371442.1±7169.4	168544.8±63974.5	0.001	HS
Area fract	0.13±0.024	0.056±0.021	0.001	HS
Area fill	0.142±0.033	0.060±0.026	0.002	HS
Area %	12.4±2.4	5.62±2.13	0.001	HS

Table (13): Comparison between III & VI study groups regarding level of liver enzymes. p-value (<0.05)

Liver enzymes	CC14 (4 Ws)	CC14 (8 Ws)	p-value	Sig.
	Mean ± SD	Mean ± SD		
ALT	68.5±11.3	90.7±9.5	0.01	HS
AST	47.5±9.2	69.9±1.9	0.002	HS
GGT	68.4±5.9	90.5±8.2	0.005	HS

Table (14): Comparison between III & VI study groups regarding degree of liver fibrosis, with p-value (<0.05).

collagen	CC14 (4 Ws)	CC14 (8 Ws)	p-value	Sig.
	Mean ± SD	Mean ± SD		
Area	371442.1±7169.4	565458.8±1.23	0.01	S
Area fract	0.13±0.024	0.19±0.043	0.02	S
Area fill	0.142±0.033	0.23±0.064	0.02	S
Area %	12.4±2.4	18.8±4.1	0.1	S

Table (15): Comparison between IV & VII study groups regarding level of liver enzymes. p-value (<0.05)

Liver enzymes	CC14 (4 Ws) & Scarification	CC14 (8 Ws) & Scarification	p-value	Sig.
	Mean ± SD	Mean ± SD		
ALT	57.9±10.5	87.4±8.6	0.002	HS
AST	36.6±3.3	63.1±5.7	>0.001	HS
GGT	48.5±12.7	83.2±12.1	0.004	HS

Table (16): Comparison between IV & VII study groups regarding liver fibrosis, p-value (<0.05).

collagen	CC14 (4 Ws) & Scarification	CC14 (8 Ws) & Scarification	p-value	Sig.
	Mean ± SD	Mean ± SD		
Area	283850.4±66930.7	467589.4±30814.1	0.001	HS
Area fract	0.094±0.023	0.154±0.008	0.001	HS
Area fill	0.108±0.027	0.186±0.012	<0.001	HS
Area %	9.46±2.22	15.6±1.02	0.001	HS

Table (17): Comparison between VI & VII study groups regarding level of liver enzymes, p-value (>0.05).

Liver enzymes (u/ml)	CC14 (8 Ws)	CC14 (8 Ws) & Scarification	p-value	Sig.
	Mean ± SD	Mean ± SD		
ALT	90.7±9.5	87.4±8.6	0.6	NS
AST	69.9±1.9	63.1±5.7	0.07	NS
GGT	90.5±8.2	83.2±12.1	0.4	NS

Table (18): Comparison between VI & VII study groups regarding degree of liver fibrosis, p-value (>0.05).

collagen	CC14 (8 Ws)	CC14 (8 Ws) & Scarification	p-value	Sig.
	Mean ± SD	Mean ± SD		
Area	565458.8±1.23	467589.4±30814.1	0.1	NS
Area fract	0.19±0.043	0.154±0.008	0.1	NS
Area fill	0.23±0.064	0.186±0.012	0.1	NS
Area %	18.8±4.1	15.6±1.02	0.1	NS

Table (19): Comparison between VI & VIII study groups regarding level of liver enzymes. p-value (<0.05)

Liver enzymes (u/ml)	CC14 (8 Ws)	CC14 (8 Ws) & MSC injection	p-value	Sig.
	Mean ± SD	Mean ± SD		
ALT	90.7±9.5	39.9±2.7	0.001	HS
AST	69.9±1.9	29.6±6	<0.001	HS
GGT	90.5±8.2	35.8±6.1	<0.001	HS

Table (20): Comparison between VI & VIII study groups regarding degree of liver fibrosis, p-value (>0.05)

collagen	CC14 (8 Ws)	CC14 (8 Ws) & MSC injection	p-value	Sig.
	Mean ± SD	Mean ± SD		
Area	565458.8±1.23	441257±41376.7	0.06	NS
Area fract	0.19±0.043	0.15±0.014	0.09	NS
Area fill	0.23±0.064	0.174±0.019	0.08	NS
Area %	18.8±4.1	14.7±1.4	0.06	NS

4. Discussion

In the present work, manifestations of the pathological impact of CCl₄ on the rat liver were recorded. Light microscopic examination revealed disrupted hepatic parenchymal architecture, dilatation and congestion of the central vein and hepatic sinusoids, increased number of Kupffer cells, inflammatory cellular infiltration, hepatocytic degeneration in the form of nuclear pyknosis, cytoplasmic vacuolation and fatty degeneration. The histomorphometric study showed increased amount of collagen fiber deposition. The electron microscopic examination demonstrated ultrastructural alterations in the form of disrupted thick plasma membrane, ballooning of mitochondria, fragmented rough endoplasmic reticulum and degenerated nucleus. Similar findings were reported by *Ren et al. (2010)* who observed that chronic exposure to CCl₄ resulted in extensive hepatic fibrosis and marked disturbance of hepatic functions.

In the present study, administration of CCl₄ for 8 weeks resulted in disrupted hepatic parenchymal architecture which was demonstrated by light microscopic examination. However, the hepatic architecture was not apparently disrupted in administration of CCl₄ for 4 weeks. This was in agreement with the findings of *Zowail, et al. (2012)* who found that light microscopic examination of liver sections of rats injected with CCl₄ at a dose of 1ml/kg twice weekly for 8 weeks showed that hepatocytes lost their normal architecture which appeared in haphazard fashion, hepatocyte swelling, variations in liver cell size and shape, that are considered precancerous lesions, and attributed these pathological changes to generation of oxygen free radicles and oxidative stress

with eventual peroxidation of membrane lipids leading to loss of hepatocellular integrity and cell surface membrane disruption. These findings were identical to observations of the present work which revealed disrupted plasma membrane of the hepatocytes. Similar findings also observed by *Kurk et al. (2000)* who stated that thromboxane B₂, that increase in CCl₄ toxicity, is responsible for plasma membrane bleb, an early event in hepatocytes injury when exposed to oxidative stress.

Thick plasma membrane has been observed in the present study. Similar findings were observed by *Mehmetcik et al. (2008)* who stated that thickening of cell surface membrane is a part of inflammatory reaction occurring in injured liver cells due to accumulation of complement C3 on the membrane.

In the current work, the degree and extent of hepatocyte lesion was observably proportionate to the duration of exposure to CCl₄; four and eight weeks durations. It showed hydropic degeneration manifested as cytoplasmic vacuolation of the hepatocytes by light and electron microscope. However, with longer duration of CCl₄ administration, the hydropic degeneration became observably marked in the form of more numerous and extensive cytoplasmic vacuolation. Similar findings were reported by *Zhu et al. (2012)* who proposed that this cytoplasmic vacuolation occurred due to increased production of toxic metabolites via activation of cytochrome P450. *Wacker et al. (2001)* reported that the nuclear damage produced by CCl₄ appears to be due to its genotoxic effect via its metabolites and lipid peroxidation products such as 4-hydroxynonenal and malondialdehyde that can bind with DNA.

In the present study, histological data of CCl₄ - treated rats revealed dilatation and engorgement of the central vein and hepatic sinusoids. These findings were moderate following CCl₄ administration for 4 weeks and became more evident with longer duration of administration of CCl₄ for 8 weeks in which additional manifestations were observed such as extravasation of blood. These results were compatible with those reported by *Yang et al. (2011)* who attributed these vascular changes to the direct toxic effect of CCl₄ on the blood vessel wall in rats.

In the current work, there was marked inflammatory cellular infiltration encountered adjoining the portal tract of the liver specimens of CCl₄ - treated group for 8 weeks. These findings could be attributed to the involvement of free radicals and oxidative stress. Similar findings were reported by *Kazeem et al. (2011)*.

In the present work, swelling of hepatocytes was observed. This was in accordance with *Newmeyer and Ferguson-Miller (2003)* who suggested that inverting of active transport system (Na⁺, K⁺- ATPase) causes

sodium to enter and accumulate inside the cells and potassium to diffuse out followed by increased water entry, leading to cellular swelling and dilatation of the endoplasmic cistern at the level of ultrastructural study.

Frequent fatty degeneration of hepatocytes was encountered in the present study, seen as accumulation of lipid vacuoles of the CCl₄ treated group for 8 weeks. This steatosis formed clear vacuoles within the cytoplasm of hepatocytes. Fatty change is often seen in the liver because it is the major organ involved in fat metabolism, resulting in triglyceride accumulation in hepatocytes (*Farrell and Larter, 2006*). The nuclei of hepatocytes of CCl₄- treated rats manifested degenerative changes as observed by both light and electron microscopic examination. These changes were moderate in CCl₄- treated rats for 4 weeks, in the form of clumping and margination of nuclear chromatin leading to karyolysis in few nuclei. However, these nuclear changes became more evident in CCl₄- treated rats for 8 weeks inducing pyknosis in which nuclei were shrunken with increased basophilia due to progressive chromatin clumping and marked degeneration of the nuclei with damage of their nucleoli and chromatin material (karyolysis). *Edinger and Thompson (2004)* attributed these nuclear changes to nonspecific breakdown of DNA while, *Golstein and Kroemer (2007)* described them as manifestations of irreversible cell damage; the nucleus might undergo progressive dissolution and the basophilia of the chromatin might fade and disappear (karyolysis), a change that reflect loss of DNA because of enzymatic degradation by endonucleases.

In the present work, mitochondrial swelling associated with partial or complete loss of cristae was found. *Whiteman et al. (2008)* stated that altered mitochondrial membrane permeability leads to an osmotic imbalance that induces the swelling and loss of cristae. Activated neutrophils release hydrogen peroxide and produce hypochlorous acid, which has been shown to cause mitochondrial dysfunction and cell death.

In the present study, depletion of the glycogen content of many hepatocytes appeared in both CCl₄-treated groups for 4 weeks and for 8 weeks as revealed by PAS reaction. This glycogen depletion could most probably be due to hepatocellular dysfunction resulting from hepatocellular injury. This explanation could be confirmed by *Kumar et al. (2009)* who stated that reduction in the oxygen supply to cells and cease of oxidative phosphorylation, result in decrease of cellular ATP and increase in adenosine monophosphate. These changes stimulate phosphor fruktokinase and phosphorylase activities, leading to an increased rate of anaerobic glycolysis, which is designed to maintain the cell's energy sources by

generating ATP through metabolism of glucose derived from glycogen are rapidly depleted. *Kumar et al. (2009)* suggested that anaerobic glycolysis results in the accumulation of lactic acid and inorganic phosphates from the hydrolysis of phosphate esters. This reduces the intracellular PH, resulting in decreased activity of many cellular enzymes.

In the current work, discontinuation of CCl₄ treatment for one month led to partial restoration of glycogen content in the liver in group IV (moderate positive PAS reaction) but it was completely depleted in group VII (faint positive PAS reaction). This was partially in agreement with *Muriel et al. (2005)* who observed in their study, that glycogen was depleted by two, three or four months of chronic intoxication with CCl₄ and discontinuation of CCl₄ treatment in two or three months led to a complete restoration of the content of glycogen in the liver.

Increased collagen fiber deposition in the liver was observed in the present study in both CCl₄-treated groups as compared to the normal control group by light microscopic examination in Masson's trichrome stained sections. On the level of histomorphometric study, the area percentage of the collagen fibers of both CCl₄- treated groups, showed statistically significant increase in their values ($P < 0.05$) as compared to the control group indicating that CCl₄ administration induced liver fibrosis. This fibrosis was more obvious with long duration of CCl₄ administration (**group V**) which showed highly significant increase in the area percent of collagen fibers of groups VII and VIII treated with MSC were much lower than those of groups (IV and V) treated only with CCl₄. The high numerical value of F- ratio indicated that the variation in the values of the measurements between the different groups was highly significant.

Normal liver has a connective tissue matrix which includes type IV collagen (non - fibrillary), glycoproteins, including fibronectin and laminin, and proteoglycans, including heparan sulphate. These constituents comprise the basement membrane in the space of Disse (*Dooley et al., 2011*). *Friedman (2008)* added that this phenotypic switch is also characterized by production of type I collagen, the high - density interstitial collagen characteristic of the cirrhotic liver, as well as matrix - degrading enzymes.

The present work showed that serum levels of liver enzymes (ALT, AST and GGT) were significantly higher ($p < 0.05$) in CCl₄- treated groups (III and VI) as compared to both normal and sham control groups in a variable degrees; this difference was higher in group VI than group III. These findings were also confirmed by *Wafeeq et al. (2012)* who reported that plasma ALT and AST activities were significantly elevated by CCl₄ as early as 3 h after

injection of CCl₄ and GGT is a more sensitive and more accurate reflector of CCl₄ induced hepatotoxicity in rats than AST. The variation in the enzyme concentration in rats treated with CCl₄ may be caused by the ability of this compound to induce hepatic cells degeneration, damage of the blood vessels in addition to the disturbance of metabolic activity of liver. There was statistically significant difference with p-value (<0.05) between group **III** and group **IV** as regards to AST and GGT liver enzymes with high mean among group **III**. On the other hand there was no statistically significant difference with p-value (>0.05) as regards to ALT level. However, in CCl₄ administration groups for eight weeks, there was no statistically significant difference with p-value (>0.05) between group **VI** and group **VII** as regards to liver enzymes. In comparison between group **IV** and group **VII** there was statistically significant difference with p-value (<0.05) between both groups as regards to liver enzymes with high mean among group **VII**. These findings were in accordance with *Gonçalves et al. (2013)* who observed in their study, but with shorter duration, that levels of these enzymes were not significantly decreased in rats treated with CCl₄ for 12 days and left for spontaneous recovery for another 12 days. In contradistinction to the results of the present study *Copple et al. (2008)* pointed out that the elevation of AST and GGT from the second to sixth week of exposure to CCl₄ followed by gradual decrease from eighth to tenth week may be explained by auto-protection which may occur either by induction of genes of some defensive enzymes or by cytochrome P2E1(CYP2E1) inactivation.

In the current work, there was statistically significant difference with p-value (<0.05) between group **IV** and group **VII** with high mean among group **VII** and between group **VI** and group **VIII** as regards to liver enzymes with high mean of group **VI**. This was in accordance with *Zhao et al. (2012)* who stated that transplantation of MSC in CCl₄- treated rats causes marked decrease in serum levels of liver enzymes and serum bilirubin more than effect of spontaneous recovery and the results were better with early treatment with MSC due to restoration of normal cellular and functional pattern of hepatocytes as result of MSC hepatic differentiation into hepatocytes.

In groups treated with CCl₄ and left for spontaneous recovery showed mild to moderate improvement of pathological features in both light and electron microscopic examination depending on the duration of exposure of animals to the drug; in group **IV** after four weeks of CCl₄ administration there was partial improvement of hepatic parenchymal architecture, congestion of the central vein and hepatic sinusoids, mitochondrial damage fragmentation of rough endoplasmic reticulum, nuclear pyknosis and

karyolysis that were observed in the pericentral area. Moderate increase in glycogen content in PAS stained sections was also encountered in this group.

Masson's trichrome stained sections showed mild to moderate increase in collagen fibers deposition around the central vein, hepatic sinusoids as well as the portal areas. This was in accordance with *Yoshiji et al. (2002)* who stated that fibrosis is a dynamic and potentially reversible process. The authors added that resolution of liver fibrosis is due to hepatic stellate cells apoptosis (that transform into fibroblasts) which play important role in pathogenesis of collagen fibers deposition, by natural killer cells and increased activity of the interstitial collagenase enzymes i.e. matrix metalloproteinases which are responsible for degradation of collagen fibers and they are expressed particularly by HSCs and Kupffer cells. However, *Kisseleva and Brenner (2012)* in their study in animal models and human liver fibrosis, indicated that interstitial collagenase enzymes activity decreases in liver extracts in advanced fibrosis that would promote net collagen deposition and irreversible liver cirrhosis that was not in agreement with the results of this study.

In the present work, the collected data of electron microscopic examination of the CCl₄ and MSC treated rats were complementary and similar to that observed by the light microscopy. In groups treated with both CCl₄ and MSC, there was disappearance of the cytoplasmic vacuolation and rarefaction in most of the observed hepatocytes. Their cytoplasm contained intact cell organelles, such as mitochondria and rough endoplasmic reticulum, which were regularly distributed throughout. However, in group **VIII** slightly ballooned mitochondria were occasionally encountered suggesting mild structural effect in this group treated with CCl₄ for 8 weeks followed by MSC administration.

In the current work, MSC administration ameliorated the light microscopic and ultrastructural alterations induced by CCl₄ exposure through differentiation of MSC into mature hepatocytes with restoration of their structural and functional activity regaining the normal hepatic parenchymal architecture. In addition, MSC administration decreased liver fibrosis. Similar findings were observed by *Fang et al. (2004)* who observed that MSC could repair CCl₄ -injured liver by reducing mononuclear cell infiltration, collagen deposition, and remodeling and MSC treatment to 4-week CCl₄ -injected rats would result in significant reduction of liver fibrosis.

CCl₄ -induced liver fibrosis was ameliorated after transplantation of MSC. These cells could ameliorate liver fibrosis by expressing certain antifibrotic factors, such as matrix metalloproteinase 9 (MMP-9) and by releasing some factors, such as soluble Kit-ligand related to the differentiation and proliferation of

transplanted MSC in liver ameliorated inflammation induced by continuous injection of CCl₄. Moreover, MSCs secrete certain growth factors, such as hepatic growth factor, nerve growth factor, and many cytokines. These have antiapoptotic activity in hepatocytes and play an essential part in the regeneration of liver (*Segovia-Silvestre et al., 2011*).

Zhao et al. (2012) reported that MMP-9 exerts active chemo tactic role in the migration of MSC towards the damaged site. Transplanted MSC resulting in the degradation of the extracellular matrix may presumably lead to improved liver function and better survival of mice. According to the reported data, increased expression of GFP⁺ cells at the site of liver injury contributed to the degradation of interstitial collagens, which has been shown by curius red staining. This collagen is degraded to gelatin, which was degraded by MMP-9 resulting in the regression of fibrosis. Contradistinction to the observed data of the present study, *Yan et al. (2009)* have demonstrated that mesenchymal stem cells display a profibrogenic propensity. Indeed, intravenously infused umbilical cord MSC contributed to the myofibroblast population (α SMA and fibroblast secretory protein-1 positive cells) in mice with CCl₄ induced liver injury.

Other possible explanations for regeneration of diseased liver and improvement of function were suggested by many authors, including the facilitation of the release of vascular endothelial growth factor from stem cells, thus, increasing the blood supply to cells and helping to repair damaged tissue (*Tang et al., 2006*). Stem cells may also act by up-regulating the Bcl-2 gene and suppressing apoptosis (*Chen et al., 2001*) or by suppressing inflammation in the diseased organ via the interleukin-6 (IL-6) pathway (*Wang et al., 2006*). Finally, hepatic stellate cells may stimulate tissue-specific stem cells, such as oval cells in the liver, facilitating regeneration of the target organ (*Austin and Lagasse, 2003*).

It could be concluded that administration of CCl₄ exert a deleterious effect on the hepatic structure and functions which was duration dependent. Intravenous injection of MSC is more suitable line of therapy than liver transplantation in end-stage liver disease.

Corresponding Author:

Maha Khaled Abd El Wahed Hussein,
Anatomy and Embryology Department, Faculty of
Medicine, Fayoum University, Egypt
E-mail: mahakhaled007@yahoo.com

References:

1. *Austin, T. W. and Lagasse, E. (2003)*: Hepatic regeneration from hematopoietic stem cells. *Mechanisms of Development*, 120:131–135.

2. *Chapell, G.; Saliva, G. O.; Uehara, T.; Pogribny, I. O. and Rusyn, I. (2016)*: Characterization of copy number alterations in a mouse model of fibrosis-associated hepatocellular carcinoma reveals concordance with human disease. *Cancer Medicine*, 5:574-585.
3. *Chen, Z.; Chua, C. C.; Ho, Y. S.; Hamdy, R. C. and Chua, B. (2001)*: Overexpression of Bcl-2 attenuates apoptosis and protects against myocardial I/R injury in transgenic mice. *The American Journal of Physiology—Heart and Circulatory Physiology*, 280: 2313–2320.
4. *Copple, I. M.; Goldring, C. E.; Kitteringham, N. R. and Park, B. K (2008)*: The Nrf2-Keap1 defense pathway: Role in protection against drug-induced toxicity. *Toxicology*, 246: 24–33.
5. *Das, S.; Hajnóczky, N.; Antony, A. N.; Csordás, G.; Gaspers, L. D.; Clemens, D. L.; Hoek, J. B. and Hajnóczky, G. (2013)*: Mitochondrial morphology and dynamics in hepatocytes from normal and ethanol-fed rats. *Pflugers Arch*, 464:101-109.
6. *Dooley, J. S.; Anna, S. F.; Lok, K. A.; Burroughs, E. and Heathcote, J. (2011)*: *Sherlock's Diseases of the Liver and Biliary System*, Twelfth ed., Blackwell Publishing Ltd., 11:103-104.
7. *Edinger, A. L. and Thompson, C. B. (2004)*: Death by design: apoptosis, necrosis and autophagy. *Curr. Cell. Biol.*, 16:663.
8. *Fang, B.; Shi, M.; Liao, L.; Yang, S.; Liu, Y. and Zhao, R. C. (2004)*: Systemic infusion of FLK1+ mesenchymal stem cells ameliorate carbon tetrachloride-induced liver fibrosis in mice. *Transplantation*, 78: 83–8.
9. *Farrell, G. C. and Larter, C. Z. (2006)*: Nonalcoholic fatty liver disease: from steatosis to cirrhosis. *J. Hepatol.*, 43:99.
10. *Friedman, S. L. (2008)*: Mechanisms of hepatic fibrogenesis. *Gastroenterology*, 134: 1655-1669.
11. *Golstein, K. and Kroemer, G. (2007)*: Death by necrosis: towards a molecular definition. *Trends Biochemical. Sci.*, 32:37.
12. *Gonçalves, R. V.; Pinto da Matta, S. L.; Novaes, R. D.; Viana, J. P. Gouveia. M. C. and Vilela. E. F. (2013)*: Bark Extract of *Bathysa cuspidata* in the Treatment of Liver Injury Induced by Carbon Tetrachloride in Rats Brazilian archives of biology and technology, international journal, 2:18.
13. *Greets, A. (2001)*: History, heterogeneity, developmental biology and functions of quiescent hepatic stellate cells. *Semin. Liver Dis.*, 21:311-335.
14. *Gurtner, G. C.; Callaghan, M. J. and Longaker MT (2007)*: Progress and potential for

- regenerative medicine. *Annu. Rev. Med.* 58: 299–312.
15. Huang, G. T.; Gronthos, S. and Shi, S. (2009): Mesenchymal stem cells derived from dental tissues vs. those from other sources: their biology and role in regenerative medicine. *J. Dent. Res.*, 88:792–806.
 16. Junqueira, L. C and Carneiro, J. (2005): Basic Histology. Text and Atlas. 11th edition. Lange Medical Book, McGraw-Hill, New York, London, pp:377-402.
 17. Karahuseyinoglu, S.; Cinar, O. and Kilic, E. (2007): Biology of stem cells in human umbilical cord stroma: in situ and *in vitro* surveys. *Stem Cells*, 25: 319-331.
 18. Kazeem, M. I.; Bankole, H. A. and Fatai, A. A. (2011): Protective Effect of Ginger in Normal and Carbon-Tetrachloride Induced Hepatotoxic Rats. *Annals of Biological Research*, 2:1-8.
 19. Kisseleva, T and Brenner, D. A. (2012): The phenotypic fate and functional role for bone marrow-derived stem cells in liver fibrosis Dept. of Medicine, University of California, San Diego, CA, USA *Journal of Hepatology*, 56: 965–972.
 20. Kierszenbaum, L. M. (2002): Liver In: Histology and cell biology: an introduction to pathology, Philadelphia, London, New York, St. Louis, Sydney and Toronto, pp.459-465.
 21. Kumar, K. M.; Abbas, A. K.; Fausto, N. and Aster, J. C. (2009): Cellular responses to stress and toxic insults: Adaptation, Injury, and Death. In: Robbins and Cotran pathological basis of disease. 8th ed., Saunders Elsevier, Philadelphia, pp.13-22.
 22. Kurk, I.; Michalska, T.; Lichtszeld, K.; Kladna, A. and Aboul-Enein, H. Y. (2000): The effect of Thymol and its derivatives on reactions generating reactive oxygen species. *Chemosphere*, 41:1059-1064.
 23. Lennon, D. P. and Caplan, A. I. (2006): Isolation of human marrow-derived mesenchymal stem cells. *Exp. Hematol.*, 34:1604–1605.
 24. Levicar, N.; Pai, M.; Habi, N. A.; Tait, P.; Jiao, L. R.; Marley, S. B.; Davis, J.; Dazi, F.; Smadja, C.; Jansen, S. L.; Nicholls, J. P.; Apperley, J. F. and Gordon, M. Y. (2008): Long-term clinical results of autologous infusion of mobilized adult bone marrow derived CD34 cells in patients with chronic liver disease. *Cell Prolif.*, 41:115-125.
 25. Lide, D. R. (2006). Handbook of chemistry and physics. 86th edition. CRC Press, Boca Raton, Florida. pp. 3–470.
 26. Manibusan, M. K.; Odin, M. and Eastmond, D. A. (2007): Postulated carbon tetrachloride mode of action: A Review. *J. Environ. Sci. and Health*, 25: 185–209.
 27. Mehmetcik, G.; Ozdemirler, N.; Kocak-Toker, U.; and Uysal, M. (2008): Effect of Pretreatment with Artichoke Extract on Carbon Tetrachloride-Induced Liver Injury and Oxidative Stress. *Experimental Toxicology Pathology*, 60: 475-480.
 28. Mohona-Rao, G.; Rao, C. V.; Pushpangadan, P. and Shirwaikar, A. (2006): Hepatoprotective effects of rubiadin, a major constituent of *Rubia cordifolia*. *J. Ethnopharmacol.*, 103: 484-490.
 29. Muriel, P.; Moreno, M. G.; Hernandez, M.; Chavez, E. and Alcantar, K. L. (2005): Resolution of Liver Fibrosis in Chronic CCl₄ Administration in the Rat after Discontinuation of Treatment: Effect of Silymarin, Silibinin, Colchicine and Trimethylcolchicinic Acid. *Basic & Clinical Pharmacology & Toxicology*, 96: 375–380.
 30. Newmeyer, D. D. and Ferguson-Miller, S. (2003): Mitochondria: releasing power for life and unleashing the machineries of death. *Cell*, 112:481.
 31. Rabani, V.; Shahsavani, M.; Gharavi, M.; Piryaei, A.; Azhdari, Z. and Baharvand, H. (2010): Mesenchymal stem cell infusion therapy in a carbon tetrachloride-induced liver fibrosis model affects matrix metalloproteinase expression. *Cell Biol. Int.*, 34: 601-605.
 32. Ren, M.; Zou, J. Y.; Gao, G. Q.; Yang, G. and Chen, R. G. (2010): Effect of bitter melon on liver fibrosis induced by carbon tetrachloride. *Chinese Journal of Pathophysiology*, 26: 2222–2225.
 33. Ross, M. H. and Pawlina, W. (2011): Liver In Histology: A text and atlas with correlated cell and molecular biology, 6th ed., Lippincott Williams & Wilkins publishers, Philadelphia, pp.532-560.
 34. Scheers, I.; Lombard, C.; Najimi, M. and Sokal, E. M. (2011): Cell Therapy for the Treatment of Metabolic Liver Disease: An Update on the Umbilical Cord Derived Stem Cells Candidates. Laboratory of Pediatric Hepatology and Cell Therapy, Brussels 1200, The Open Tissue Engineering and Regenerative Medicine Journal, 4:48-53.
 35. Segovia-Silvestre, T.; Reichenbach, V.; Fernández-Varo, G.; Vassiliadis, E.; Barascuk, N.; Morales-Ruiz, M.; Karsdal, M. A. and Jiménez, W. (2011): Circulating CO3-610, a degradation product of collagen III, closely reflects liver collagen and portal pressure in rats with fibrosis. *Fibrogenesis & Tissue Repair*, 4:19.
 36. Stevens, A. and Lowe, J. S. (2005): Liver In: Human histology, 3rd ed., Elsevier Mosby, Philadelphia, Edinburgh, London, New York,

- Oxford, St. Louis, Sydney and Toronto, pp.229-236.
37. Smyth, R.; Munday, M. R.; York, M. J.; Clarke, C. J.; Dare, T. and Turton, J. A. (2007): Comprehensive characterization of serum clinical chemistry parameters and the identification of urinary superoxide dismutase in a carbon tetrachloride-induced model of hepatic fibrosis in the female Hanover Wistar rat. *Int. J. Exp. Pathol.*, 88: 361-376.
 38. Takami, T.; Terai, S. and Skadia, I. (2014): Advanced therapies using autologous bone marrow cells for chronic liver disease. *Discovery Medicine*, 14:7-12.
 39. Tang, J.; Xie, Q.; Pan, G.; Wang, J. and Wang, M. (2006): Mesenchymal stem cells participate in angiogenesis and improve heart function in rat model of myocardial ischemia with reperfusion. *European Journal of Cardio-thoracic Surgery*, 30:353-361.
 40. Théard, D.; Steiner, M.; Kalicharan, D.; Hoekstra, D. and Van, S. C. (2007): Cell Polarity Development and Protein Trafficking in Hepatocytes Lacking E-Cadherin/ β -Catenin-based Adherens Junctions *Mol. Biol. Cell*, 18: 2313-2321.
 41. Wacker, M.; Wanek, P. and Eder, E. (2001): Detection of 1, N2-propanodeoxyguanosine adducts of *trans*-4-hydroxy- 2-nonenal after gavage of *trans*-4-hydroxy-2-nonenal or induction of lipid peroxidation with carbon tetrachloride in F344 rats. *Chem. Biol. Interact.*, 137: 269-283.
 42. Wafeeq, N. H.; Maha, k. I. and Abdulah, H. L. (2012): Histological and Biochemical study on effect of dried fruit extract of *S. nigrum* on Hepatopathy induced by CCL4. *Basrah Journal of Scienc*, 30:94-104.
 43. Walker, S. J.; Weiss, R. F. and Salameh. P. K. (2001): Reconstructed histories of the annual mean atmospheric mole fractions for the halocarbons CFC-11, CFC-12, CFC-113 and carbon tetrachloride. *Journal of Geophysical Research*, 105: 14285-96.
 44. Wang, M.; Tsai, B. M.; Crisostomo, P. R. and Meldrum, D. R. (2006): Pretreatment with adult progenitor cells improves recovery and decreases native myocardial proinflammatory signaling after ischemia. *Shock*, 25: 454-459.
 45. Whiteman, M.; Spencer, J. P.; Szeto, H. H. and Armstrong, J. S. (2008): Do mitochondriotropic antioxidants prevent chlorinative stress-induced mitochondrial and cellular injury?. *Antioxid. Redox. Signal*, 10: 641-650.
 46. Xiao, J.; Liang, E. C. Ling, M.; Ching, Y.; Fung, M. and Tipoe. G. L. (2012): S-allylmercaptocysteine reduces carbon tetrachloride-induced hepatic oxidative stress and necroinflammation via nuclear factor kappa B-dependent pathways in mice. *Eur. J. Nutr.*, 51: 323-333.
 47. Yang, X.; He, X.; He, J.; Zhang, L.; Su, X. J.; Dong, Z. Y.; Xu, Y. J.; Li, Y. and Li, Y. (2011): High efficient isolation and systematic identification of human adipose-derived mesenchymal stem cells. *J. Biomed. Sci.*, 18: 27-59.
 48. Yan, Y.; Xu, W. and Qian, H. (2009): Mesenchymal stem cells from huma umbilical cords ameliorate mouse hepatic injury *in vivo*. *Liver Int.*, 29: 356-365.
 49. Yoshiji, H.; Kuriyama, S.; Yoshii, J.; Ikenaka, Y.; Noguchi, R.; Nakatani, T.; Tsujinoue, H.; Yanase, K.; Namisaki, T.; Imazu, H.; and Fukui, H. (2002): Tissue Inhibitor of Metalloproteinases-1 Attenuates Spontaneous Liver Fibrosis Resolution in the Transgenic Mouse. *Hepatology*, 36:850-860.
 50. Zhao, W.; Li, J.; Cao, D.; Li, X.; Zhang, L.; He, Y.; Yue, S.; Wang, D. and Dou, k. (2012): Intravenous injection of mesenchymal stem cells is effective in treating liver fibrosis. *World J. Gastroenterol.*, 18: 1048-1058.
 51. Zhu, R. Z.; Xiang, D.; Xie, C.; Li, J. J.; Hu, J. J.; He, H. L.; Yuan, Y. S.; Gao, J.; Han, W. and Yu, Y. (2010): Protective effect of recombinant human IL-1Ra on CCl4-induced acute liver injury in mice. *World J. Gastroenterol.*, 16:2771-2779.
 52. Zhu, H.; Jia, Z. Q.; Hara, M. and Li, Y. R. (2012): Oxidative stress and redox signaling mechanisms of alcoholic liver disease: Updated experimental and clinical evidence. *J. Digest. Dis.*, 13: 133-142.
 53. Zowail, M.; Waer, H. F.; Eltahawy, N. A.; Khater, E. H. and Abd El-hady, A. M. (2012): Curative Effect of Bone Marrow Cells Transplantation and/or Low Dose Gamma Irradiation on Liver Injuries Induced by Carbon Tetrachloride. *The Egyptian Journal of Hospital Medicine*, 46: 96 - 114.